SAND2012-3535 C

SAND2012-3535C

Metallography, 3D Reconstructions & kinetic Monte Carlo

J. Madison[1], L. K. Aagesen[2] , V. Tikare[3], E. Holm[1],

[1]SNL, Computational Material Science & Engineering, Albuquerque, NM

[2]University of Michigan, Material Science & Engineering, Ann Arbor, MI

[3]SNL, Advanced Nuclear Fuel Cycle Technologies, Albuquerque, NM

LOCKHEED MARTIN

Sandia National Laboratories

Sandia National Laboratories is a multi-program laboratory managed and operated by Sandia Corporation, a wholly owned subsidiary of Lockheed Martin Corporation, for the U.S. Department of Energy's National Nuclear Security Administration under contract DE-AC04-94AL85000.

Acknowledgements

- Sandia National Laboratories, Albuquerque, NM
  - Danny O. Maccallum, Org. 1831 – Multiscale Metallurgical S&T
  - Joseph A. Romero, Org. 1522 – Experimental NDE & Model Validation
  - Burke L. Kernen, Org. 1522 – Experimental NDE & Model Validation
  - Alice Kilgo, Org. 1822 – Materials Characterization
  - John Emery, Org. 1524 – Solid Mechanics
  - James Foulk, III, Org. 8256 – Mechanics of Materials
  - Bethany Lust, Org. 1814 – Computational Materials

- Naval Research Laboratory
  - Dave Rowenhorst, Multifunctional Materials Division

- Sandia National Laboratories, Early Career LDRD Award

Outline

- Background
  - Sandia History; Evolving Mission; People; Disciplines & Thrusts
  - 3-Dimensionality (Characterization & Modeling)
- Interrogation Methods (Benefits & Challenges)
  - Length Scale
  - Destructive/Non-Destructive
  - Labor Intensity
  - Data Acquisition Time
- Weld Characterization
  - Mechanical Sectioning
  - Ultrasonic Scan
  - Micro-Computed Tomography
- Summary
- Future Work

Sandia's History

exceptional service in the national interest.

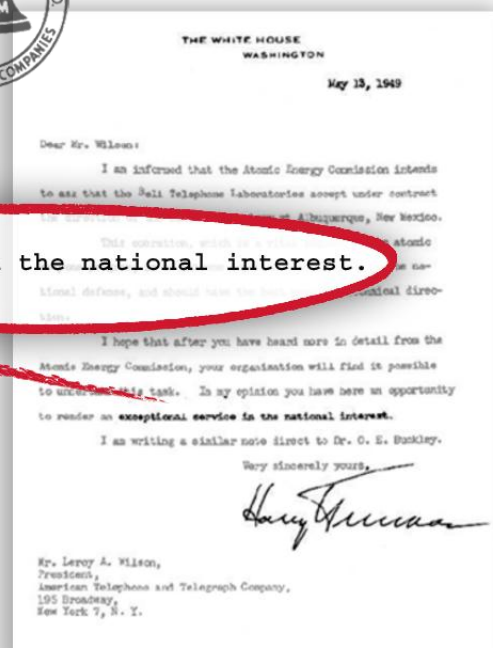

THE WHITE HOUSE
WASHINGTON

May 13, 1949

Dear Mr. Wilson:

I am informed that the Atomic Energy Commission intends to ask that the Bell Telephone Laboratories accept under contract [illegible] at Albuquerque, New Mexico.

[illegible] atomic [illegible] na- tional defense, and should have the [illegible] nical direc- tion.

I hope that after you have heard more in detail from the Atomic Energy Commission, your organization will find it possible to under[illegible] this task. In my opinion you have here an opportunity to render an **exceptional service in the national interest.**

I am writing a similar note direct to Dr. O. E. Buckley.

Very sincerely yours,

Harry Truman

Mr. Leroy A. Wilson,
President,
American Telephone and Telegraph Company,
195 Broadway,
New York 7, N. Y.

Sandia National Laboratories

SNL's Evolving Mission

1950s	1960s	1970s	1980s	1990s	2000s
Production engineering & manufacturing engineering	Development engineering	Multiprogram laboratory	Research, development and production	Post-Cold War transition	Broader national security challenges

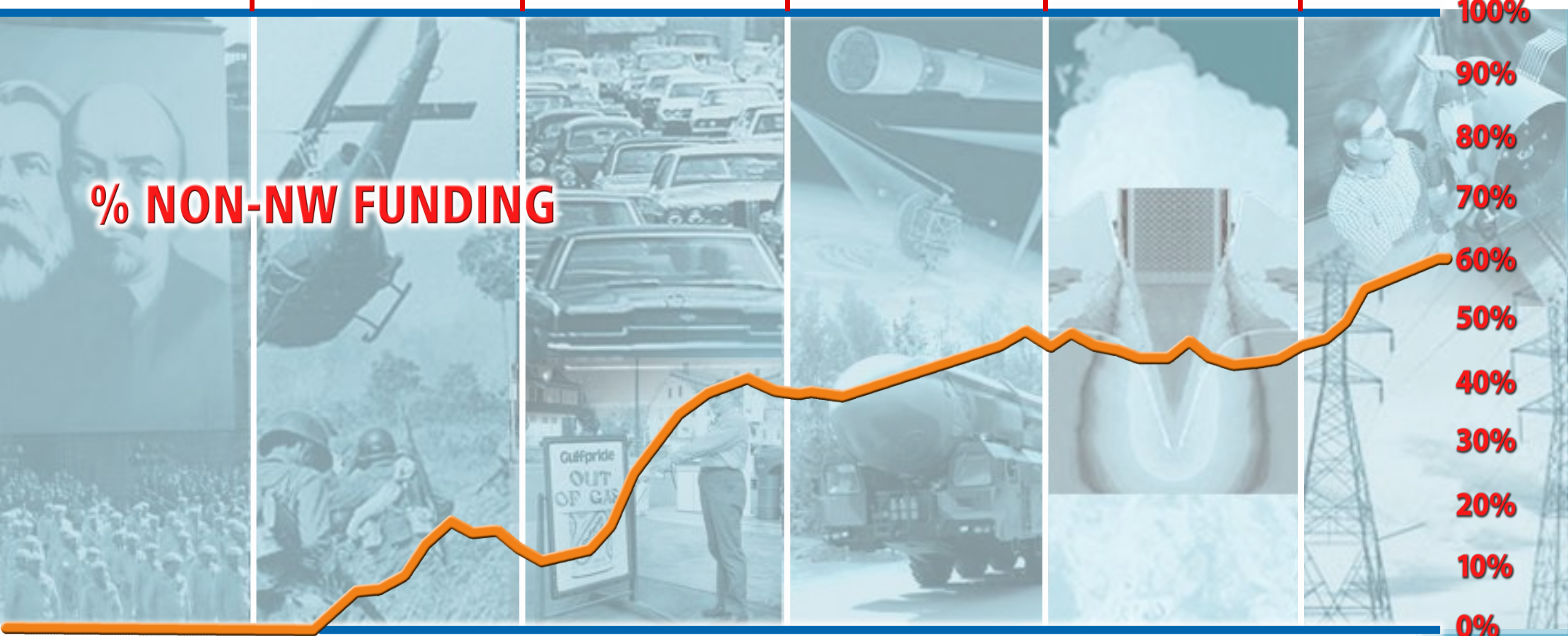

Sandia National Laboratories

People & Budget (FY 2010)

- On-site workforce: 11,677
- Regular employees: 8,607
- Gross payroll: ~ $898.7 million

FY10 operating revenue
$2.3 billion

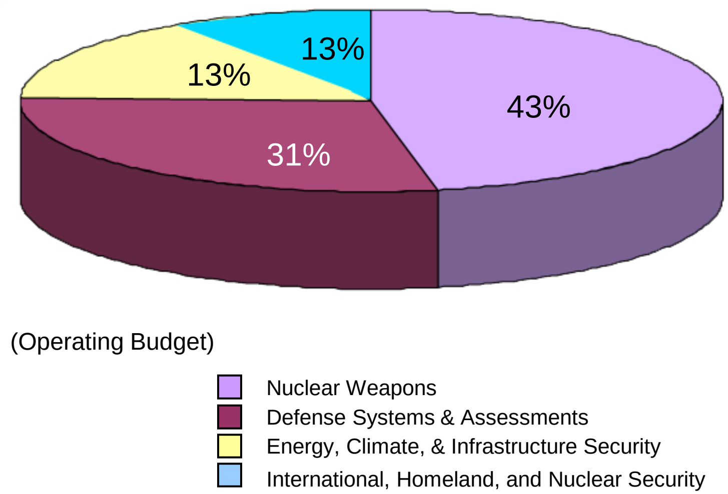

Technical staff (4,277) by discipline:

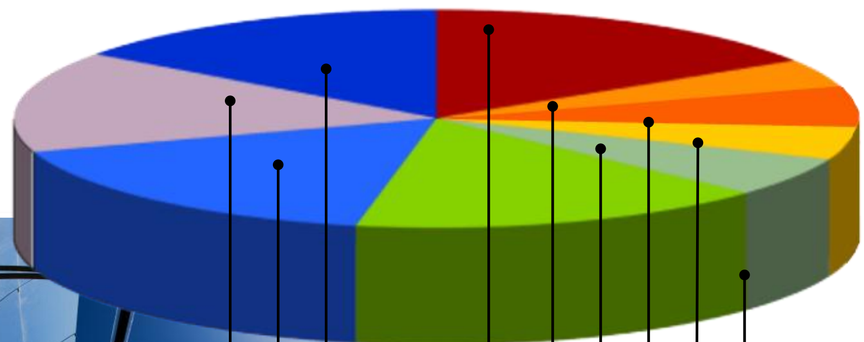

R&D Disciplines & Capabilities

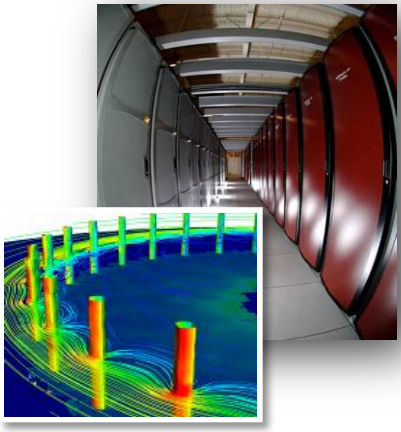

High Performance Computing

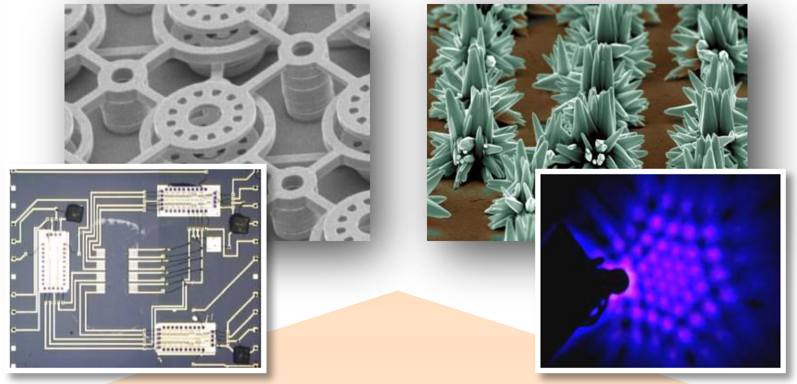

Nanotechnologies & Microsystems

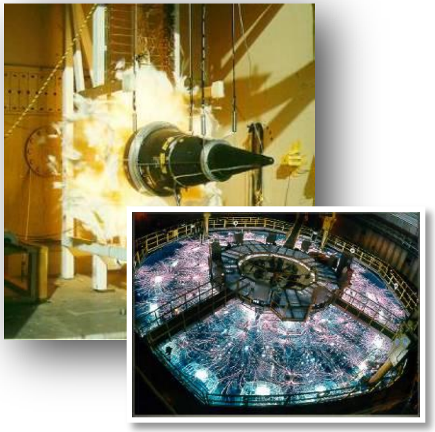

Extreme Environments

COMPUTER SCIENCE	MATERIALS	ENGINEERING SCIENCES	MICRO ELECTRONICS	BIOSCIENCE	PULSED POWER
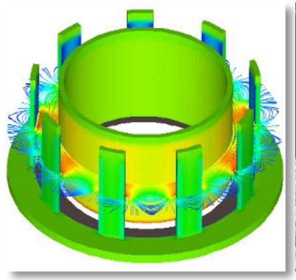	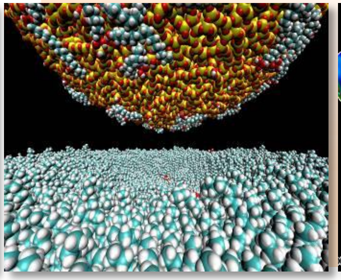	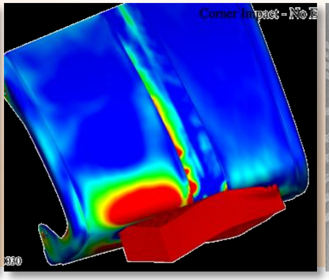	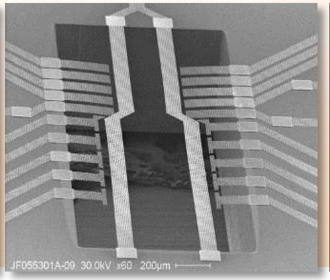	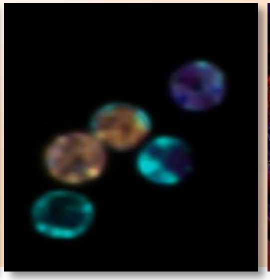	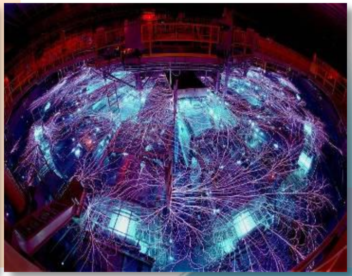

RESEARCH DISCIPLINES

National Security Thrusts

Nuclear

Energy

Cyber

Science & Technology

3-Dimensionality

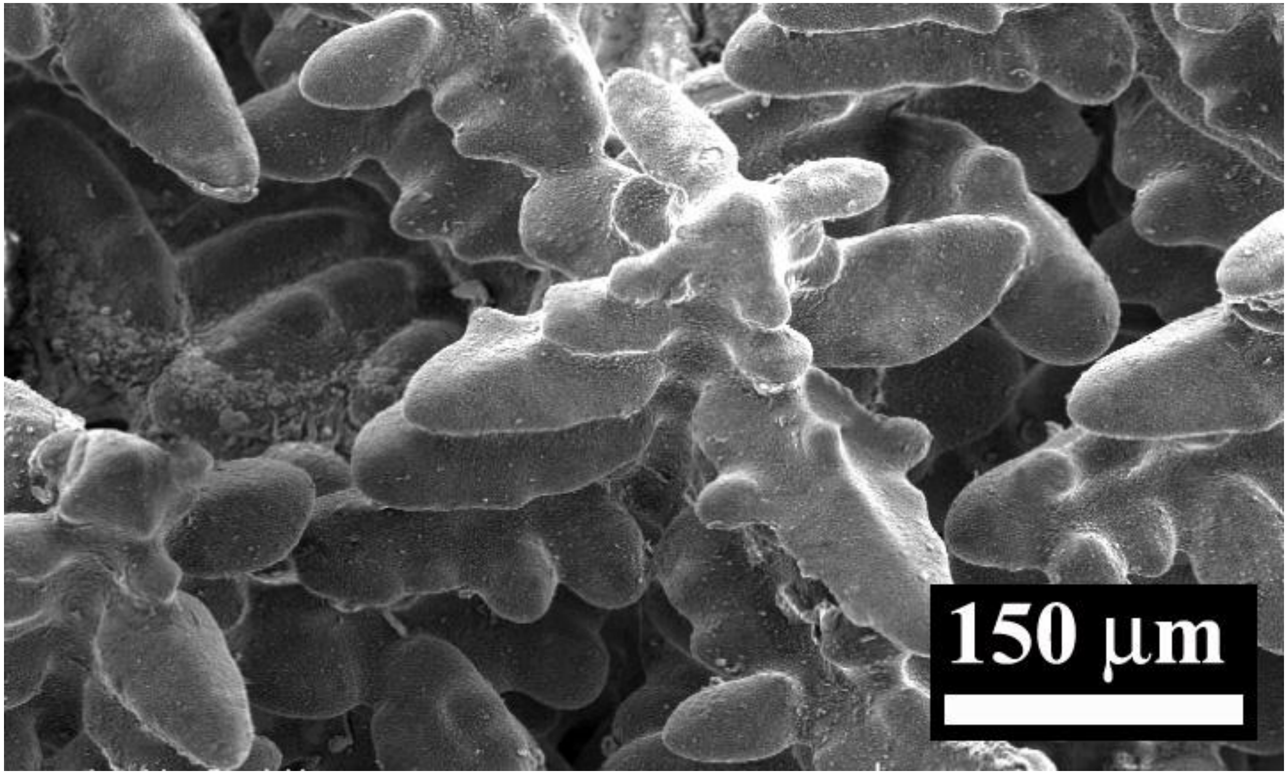

J. Madison *et al., "Fluid Flow and Defect Formation in the Three-Dimensional Dendritic Structure of Nickel-Based Single Crystals"* **Metallurgical & Materials Transactions A** doi: 10.1007/s11661-011-0823-8

J. Madison *et al., "Modeling Fluid Flow in Three-Dimensional Single Crystal Dendritic Structures"* **Acta Materialia** 58 (2010) pp. 2864 – 2875

Characterization > Modeling

Liquid Representations

Ni-Al-W Ternary | **René N4**

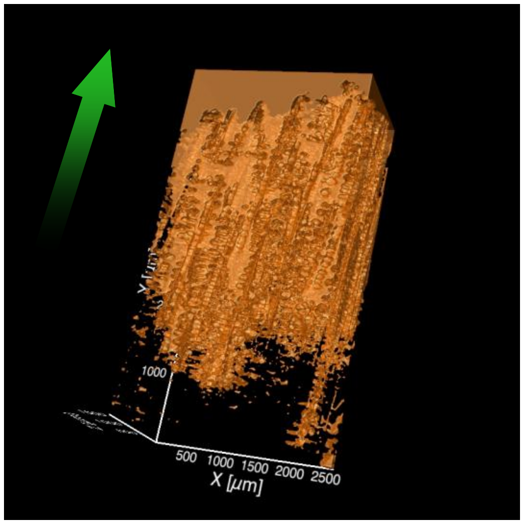

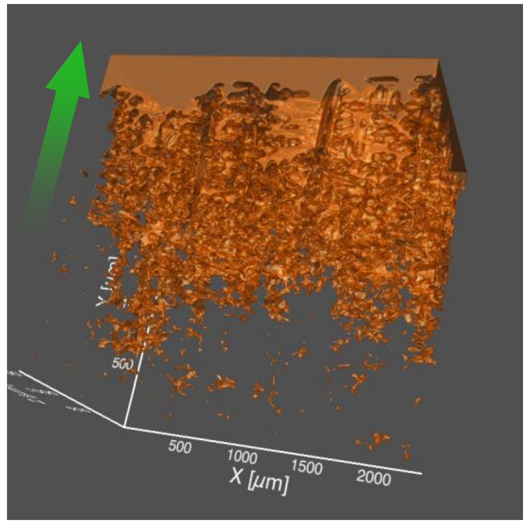

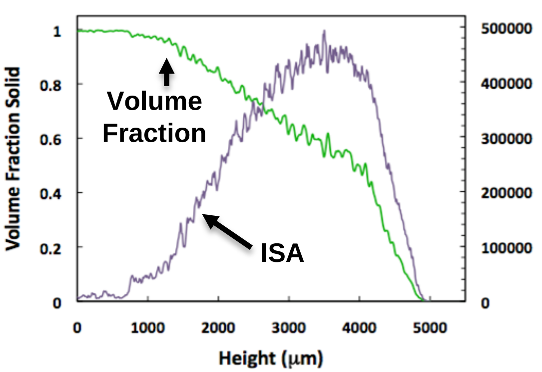

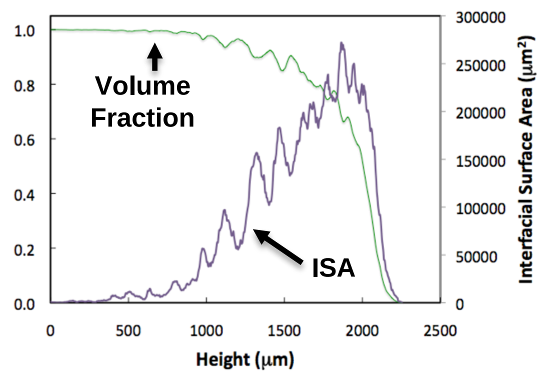

- 3D reconstructions at the dendritic front in two experimentally derived nickel-base superalloy systems
- Characterization including direct measurement of interfacial surface area providing indication of its effect on flow
- Simulation of 3D fluid flow parallel (K_y), and normal (K_x), to the primary growth direction as functions of volume fraction.

FLUENT

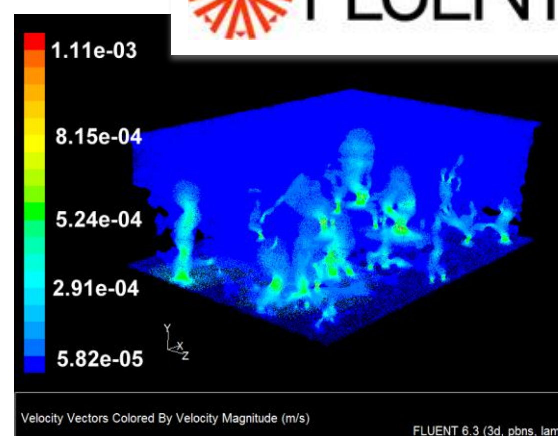

Sandia National Laboratories

Models > Predictors

$$Ra = \frac{(\Delta\rho/\rho_o)gKh}{\alpha\nu}$$

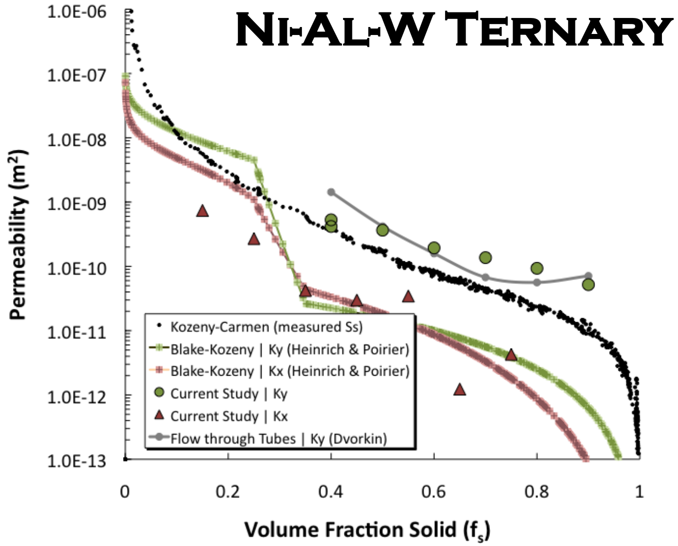

- Decreases in permeability coincide with increased tortuosity only in vertical flow (K_y)

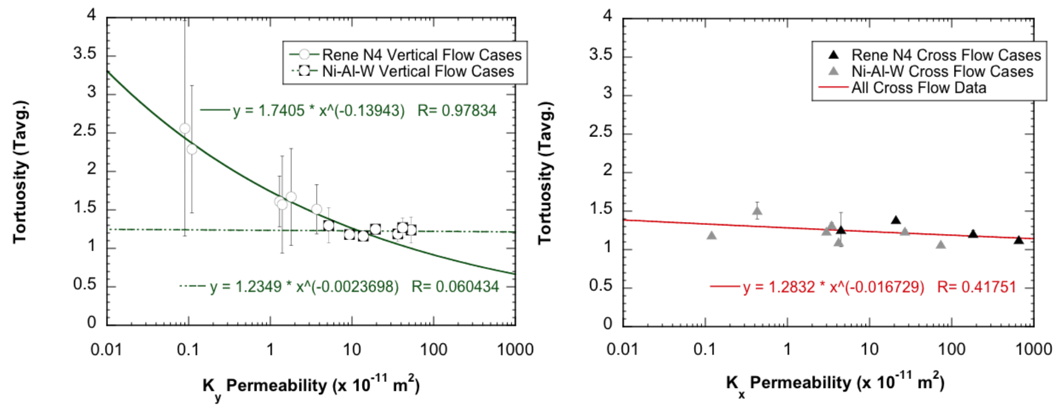

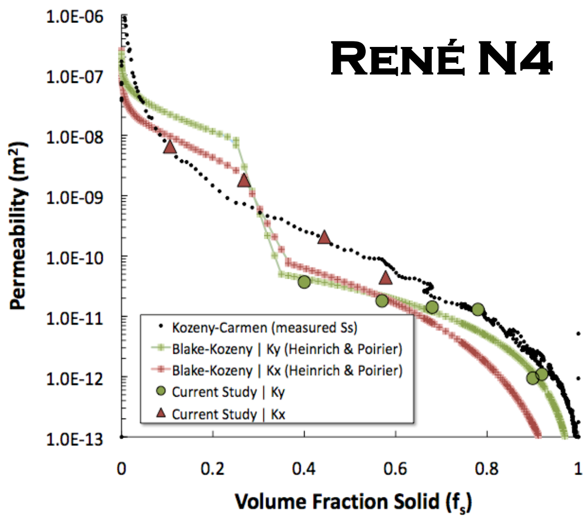

- Permeability scales inversely with S_V in both vertical and cross flow (K_y) regardless of volume fraction

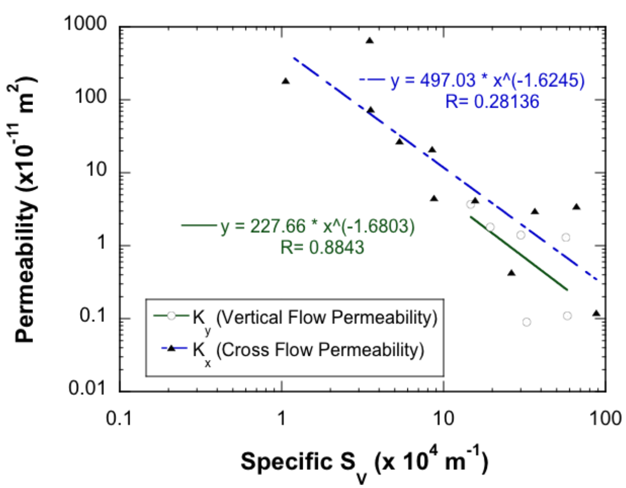

Why Study Microstructure in 3D

- Typical imaging techniques which view 2-Dimensional sections can be inadequate for determining accurate internal 3-Dimensional microstructure
  - Many mistakes in past literature have been revealed in recent 3D studies

- 3-Dimensional shapes & distributions of morphologies:
  - Strongly influence mechanical properties of materials
  - Critical to predictive models for materials response

- Importance of 3-Dimensional analysis in materials science is well known and receiving increasing attention
  - (*e.g. Scripta Materiala,* 2006, vol. 55, no. 1)
  - *(e.g. JOM,* 2006, vol. 58, no. 12)
  - (*e.g. MRS Bulletin*, 2008 vol. 33, no. 6)
  - (e.g. *JOM, 2011*, vol. 63, no. 3 & no. 7)
  - (Int’l Congress on 3D Materials Science, Seven Springs 2012)

- Ability to combine imaging (and machining) modes for interrogation of materials to specifically address materials problems is unprecedented

Interrogation Methods

	Length scales (m)	Destructive (D/ND)	Labor Intensity	Data Acquisition Time
Atom Probe Tomography [APT]	$10^{-10} – 10^{-8}$	D	Medium	Medium
Focused Ion Beam Milling [FIB]	$10^{-8} – 10^{-5}$	D	Low	Medium
Mechanical Sectioning [MecS]	$10^{-7} – 10^{-3}$	D	High	High
3DXray Diffraction [3DXRD]	$10^{-6} – 10^{-3}$	ND	High	High
Micro-Computed Tomography [μCT]	$10^{-6} – 10^{-3}$	ND	Low	Low
Femto-second Laser Sectioning [FSL]	$10^{-5} – 10^{-3}$	D	Low	Low
Ultrasonic Testing Scan [UTC]	$10^{-5} – 10^{-1}$	ND	Low	Low

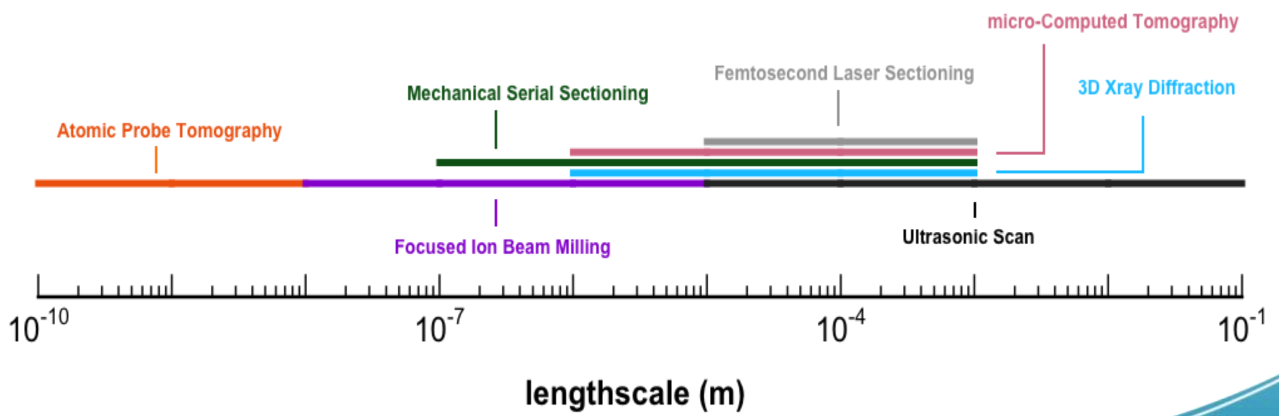

Interrogation Methods

	Obtainable Data	References
Atom Probe Tomography [APT]	*(in-situ)* material absence, elemental composition, inclusion identification	Y. Amouyal, D.N. Seidman, ***Acta Mat.,*** 2011, in press D. Isheim, ***Scripta Mater.,*** 2006, p. 35S D. Seidman, et al. ***JOM,*** 2006, p. 34
Focused Ion Beam Milling [FIB]	*(in-situ)* material absence, crystallography, inclusion identification	M. Uchic, et al., ***Scripta Mater.,*** 2006, p. 23 M. Uchic, et al., ***Ultramicroscopy,*** 2009, p. 1229 M. Uchic, ***JOM,*** 2006, p. 24
* Mechanical Sectioning [MecS]	material absence, crystallography, inclusion identification	J. Spowart, ***Scripta Mater.,*** 2006, p. 5 G. Spanos, et al. ***MRS Bulletin,*** 2008, p. 597 D. Rowenhorst, ***JOM***, 2011, p. 53
3DXray Diffraction [3DXRD]	material absence, crystallography, inclusion identification	E. Lauridsen, et al., ***Scripta Mater.,*** 2006, p. 51 D. Juul Jensen, et al., ***MRS Bulletin,*** 2008, p. 621 E. Lauridsen, et al. ***JOM***, 2006, p. 40
* Micro-Computed Tomography [μCT]	material absence	J. Baruchel, et al., ***Scripta Mater.,*** 2006, p. 41 J.-Y. Buffiere et al., ***MRS Bulletin,*** 2008, p. 611
Femto-second Laser Sectioning [FSL]	material absence, crystallography, inclusion identification	M. Echlin, et al., ***Adv. Mater.***, 2011, p. 2339
* Ultrasonic Testing Scan [UTC]	material absence	A.S. Birks & R.E. Green, Ultrasonic Testing (NDT Handbook) vol. 7, ASND, 1991

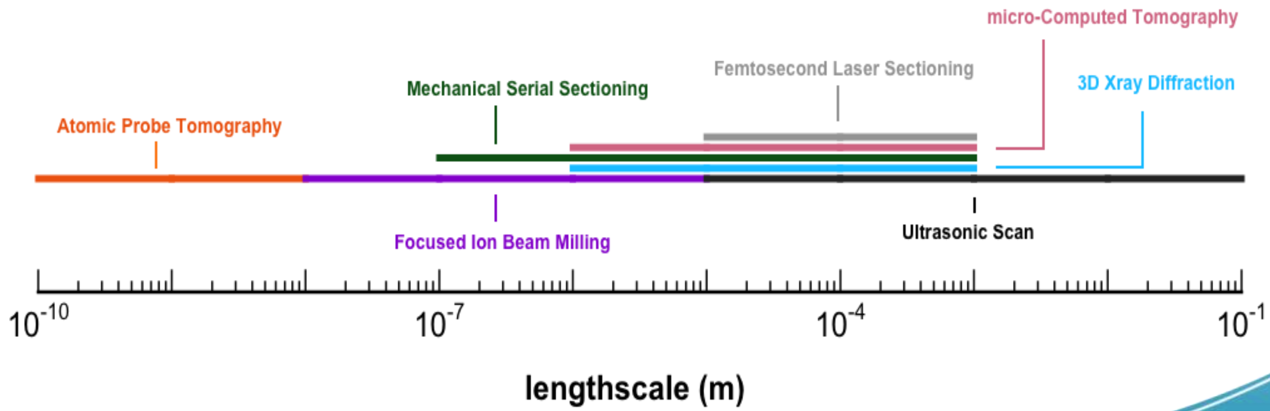

Part I

3D Characterization of Weld Microstructures in 304L Stainless Steel

Weld Applicability to SNL

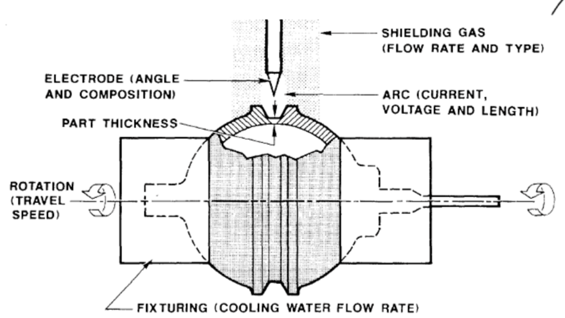

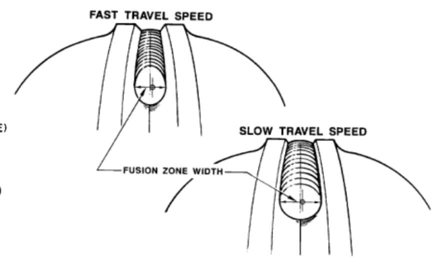

A. Bentley, **SAND2002-4014** : Feedback Control of Arc Welding Using Quantitative Feedback Theory, February 1991

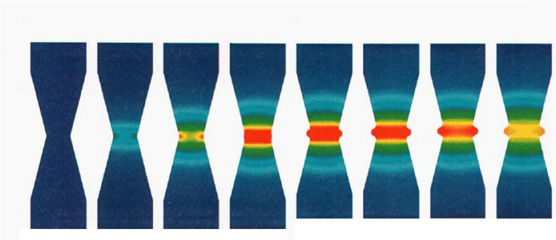

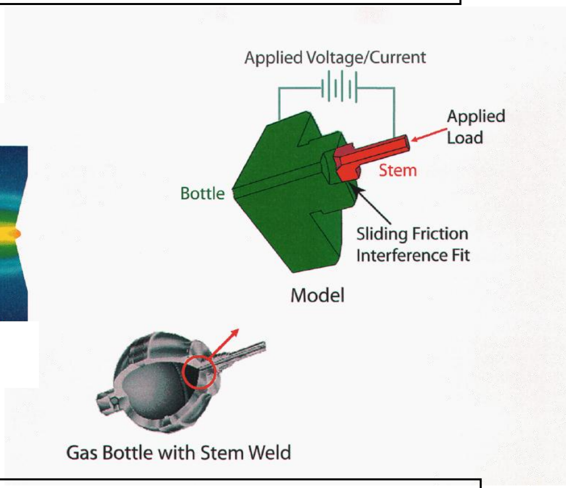

W. Winters, A. Brown, D. Bammann, J. Foulk III, A. Ortega, **SAND2005-3000:** Progress Report for the ASCI AD Resistance Weld Process Modeling Project AD2003-15, May 2005

- M. Cieslak, A. Ritter, "Precipitate Formation in Austenitic Stainless Steel Welds," **Scripta Met.**, Vol. 19, Issue 2, (1985) pp. 165-168
- J. Jellison, M. Cieslak, *Laser Materials Processing at Sandia National Laboratories,* presented at Applications of Lasers and Electro-Optics, Orlando FL, October 1994
- J. Knorovsky, M. Kanouff, P. Fuerschbach, D. Noble, P. Schunk, D. MacCallum, Hooper, *Calculated versus experimental heat inputs in laser spot welding,* presented at The American Welding Society, Chicago IL, April 2000
- C. Robino, A. Hall, J. Brooks, T. Headley, R. Roach, **SAND2002-4014** : Solidification Diagnostics for Joining and Microstructural Simulations, January 2003
- V. Semak, G. Knorovsky, D. MacCallum, R. Roach, "Effect of Surface Tension on Melt Pool Dynamics During Laser Pulse Interaction," **J. Phys. D: Appl. Phys.** Vol. 39, (2006) pp. 590-595
- *Boyce, Reu & Robino, The Constitutive Behavior of Laser Welds in 304L Stainless Steel Determined by Digital Image Correlation, **Met Trans A,** Vol. 37A (2006) pp. 2481-2492*
- J. Norris, M. Perricone, R. Roach, K. Faraone & C. Ellison, **SAND2007-1051** : Evaluation of Weld Porosity in Laser Beam Seam Welds: Optimizing Continuous Wave and Square Wave Modulated Processes, February 2007

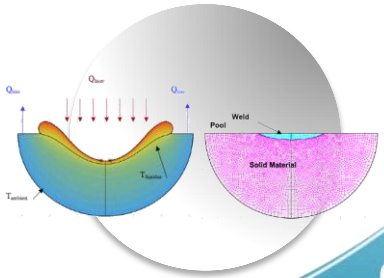

Sandia National Laboratories

Effect of Porosity

INSTITUTE OF PHYSICS PUBLISHING JOURNAL OF PHYSICS D: APPLIED PHYSICS
J. Phys. D: Appl. Phys. **38** (2005) 722–728 doi:10.1088/0022-3727/38/5/009

Porosity reduction in Nd–YAG laser welding of stainless steel and inconel alloy by using a pulsed wave

T Y Kuo[1] and S L Jeng[2]

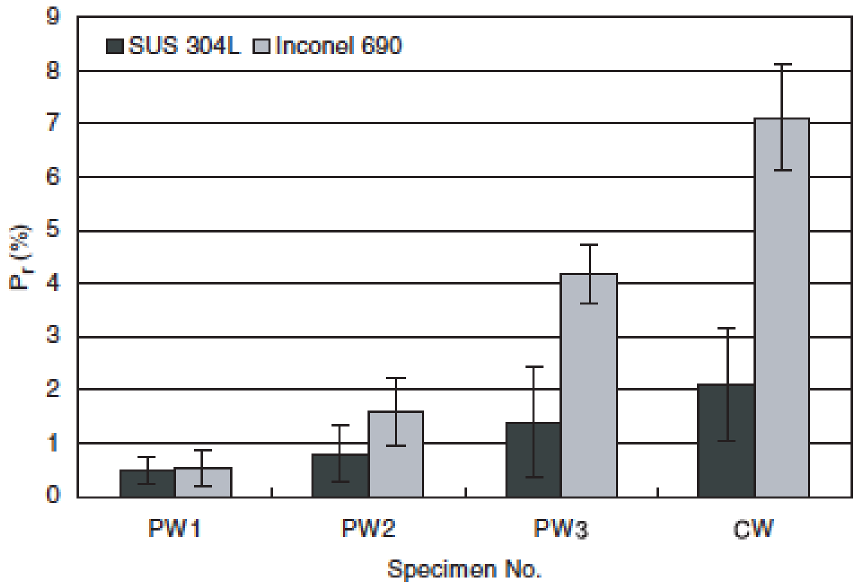

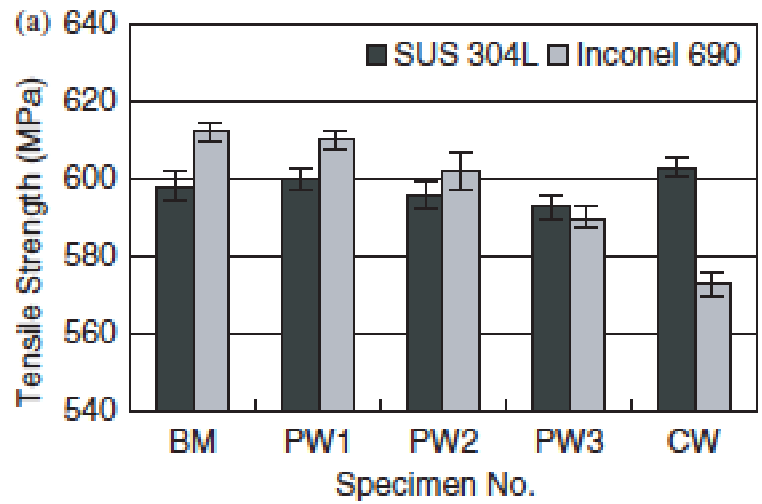

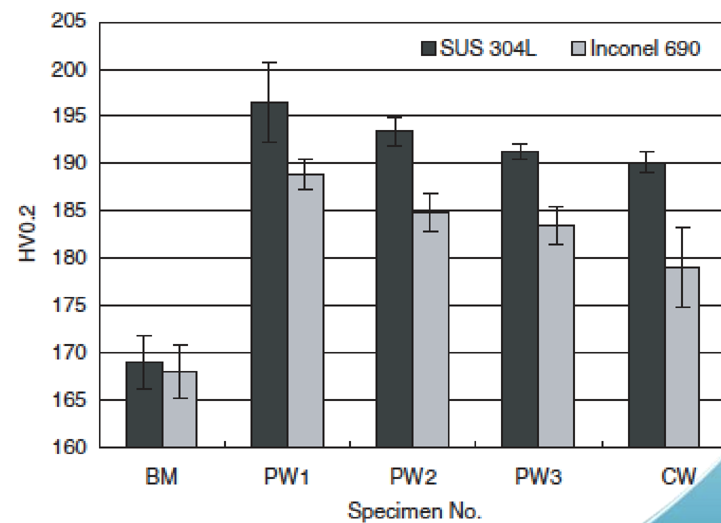

Kuo and Jeng, Porosity Reduction in Nd-YAG Laser Welding of Stainless Steel and Inconel Alloy by Using a Pulsed Wave, ***J. Phys. D: Appl. Phys.,*** *Vol. 38 (2005) pp. 722-728*

Sandia National Laboratories

Welds Examined I

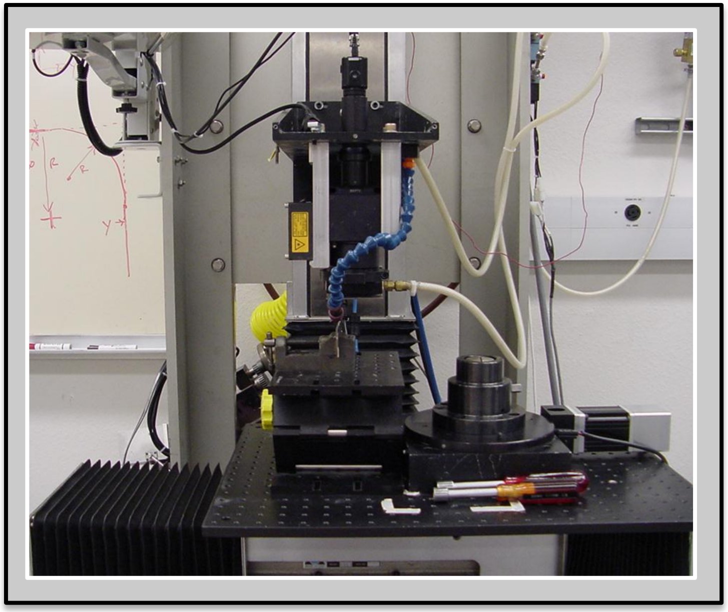

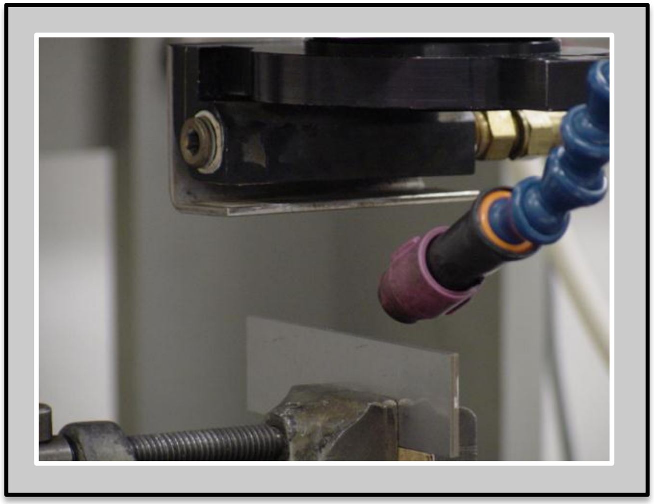

C	Cr	Cu	Mn	Mo	Ni	N	P	S	Si	Fe
0.03	18.09	0.2	1.73	0.16	8.57	0.06	0.024	0.001	0.36	bal.

304L Stainless Steel (wt%)
HEAT 2

C	Cr	Cu	Mn	Mo	Ni	N	P	S	Si	Fe
0.024	18.2	0.42	1.83	0.16	8.3	0.041	0.03	0.001	0.45	bal.

304L Stainless Steel (wt%)
HEAT 1

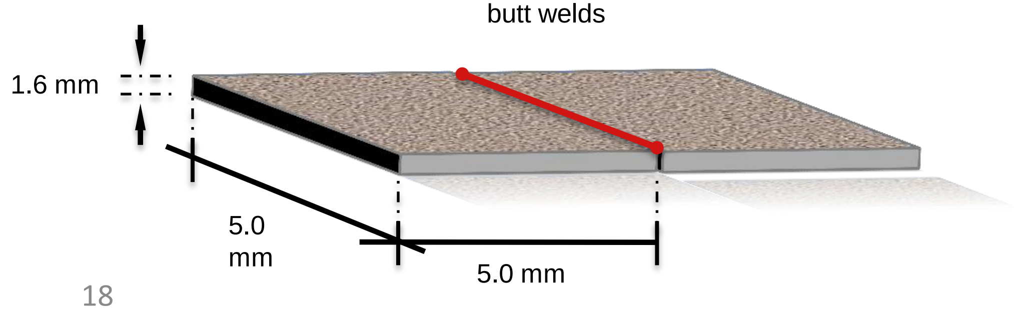

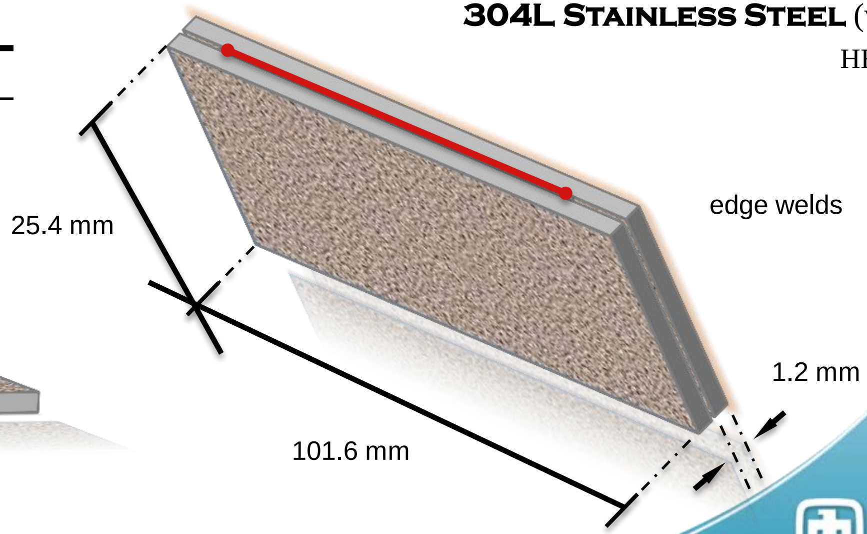

Sandia National Laboratories

Welds Examined II

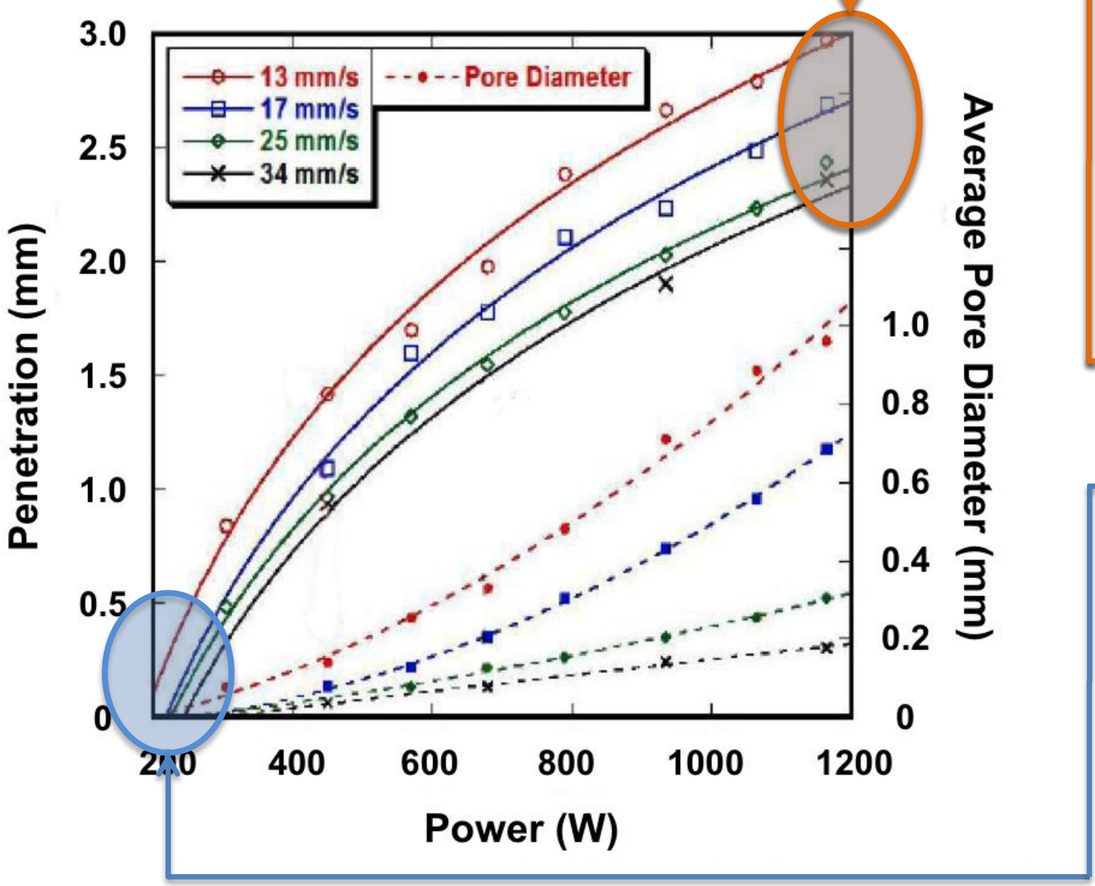

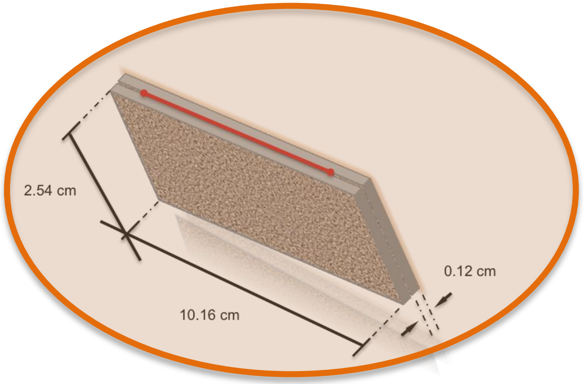

edge joint welds

butt joint welds

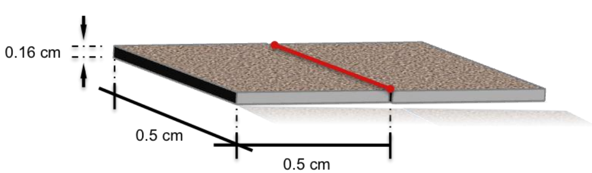

J. Norris, et al. Evaluation of Weld Porosity in Laser Beam Seam Welds: Optimizing Continuous Wave and Square Wave Modulated Processes. ***SANDIA REPORT*** *SAND2007-1051 (2007)*

Metallography

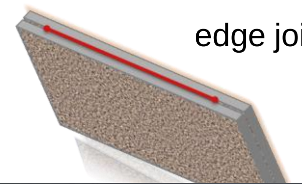

edge joint

Quantity	Lens	Power (Measured)	Speed
(2)	80 mm	1200 W	40"/min
(2)	80 mm	1200 W	60"/min
(2)	80 mm	1200 W	80"/min
(2)	120 mm	1200 W	40"/min
(2)	120 mm	1200 W	60"/min
(2)	120 mm	1200 W	80"/min

Material: 304L Stainless Steel
Heat : 481361 (1.92 Cr/Ni)
Laser: Rofin Nd:YAG

Sandia National Laboratories

Metallography

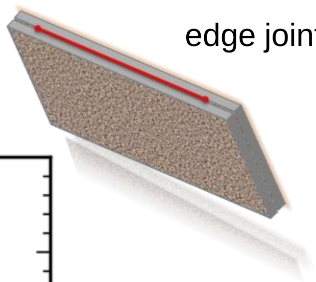

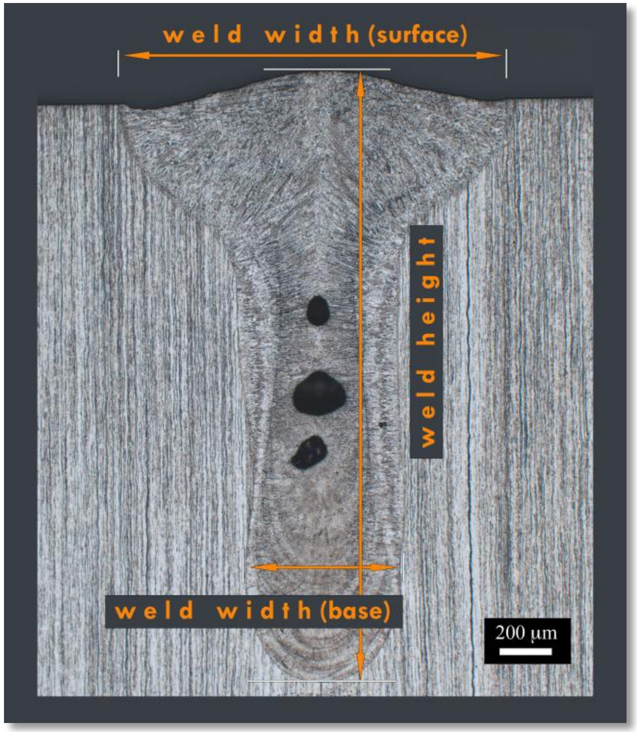

Quantity	Lens	Power (Measured)	Speed
(2)	80 mm	1200 W	40"/min
(2)	80 mm	1200 W	60"/min
(2)	80 mm	1200 W	80"/min
(2)	120 mm	1200 W	40"/min
(2)	120 mm	1200 W	60"/min
(2)	120 mm	1200 W	80"/min

Material: 304L Stainless Steel
Heat : 481361 (1.92 Cr/Ni)
Laser: Rofin Nd:YAG

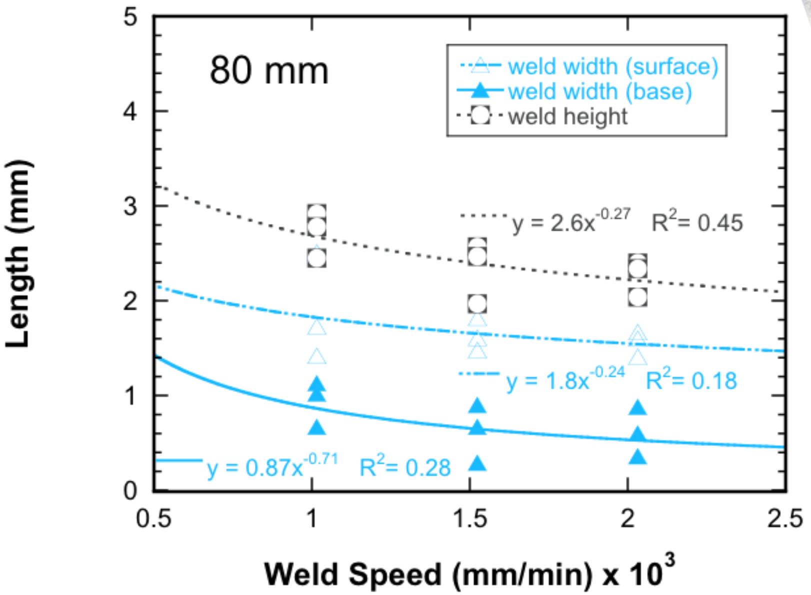

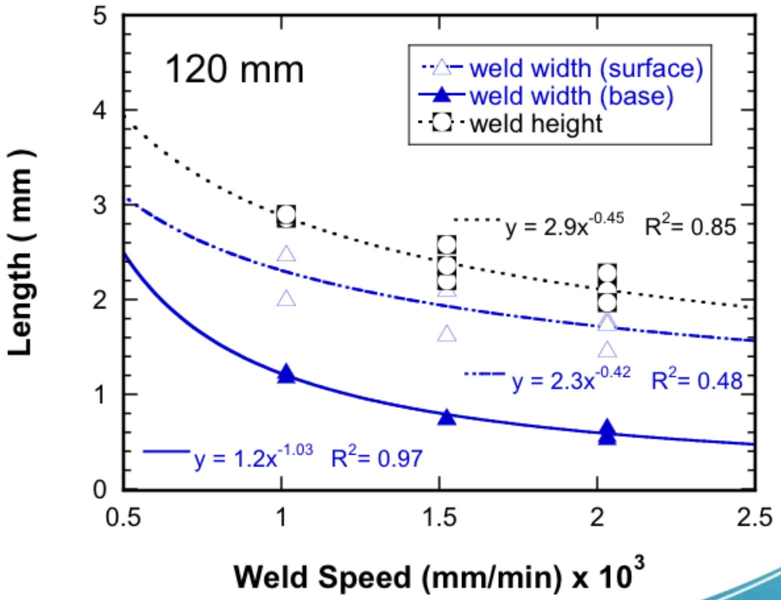

Metallography

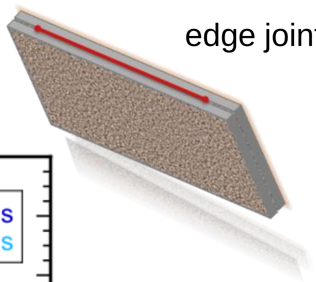

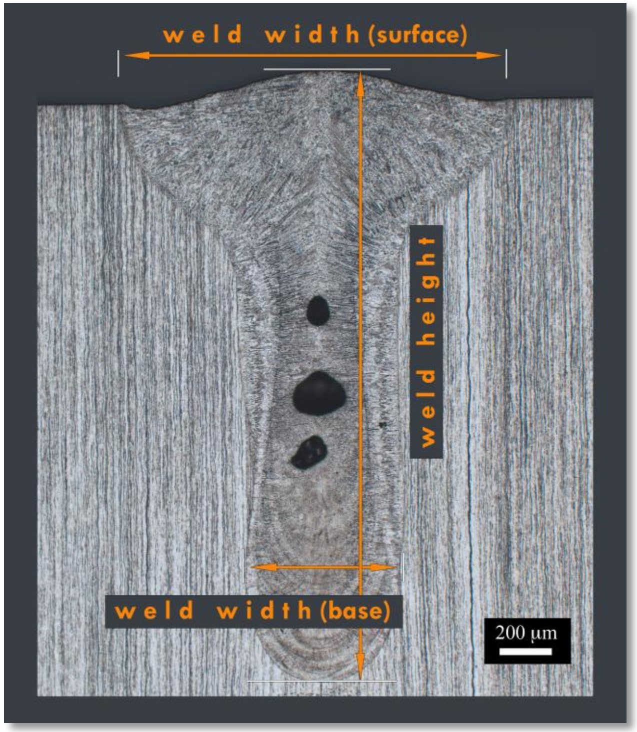

Quantity	Lens	Power (Measured)	Speed
(2)	80 mm	1200 W	40"/min
(2)	80 mm	1200 W	60"/min
(2)	80 mm	1200 W	80"/min
(2)	120 mm	1200 W	40"/min
(2)	120 mm	1200 W	60"/min
(2)	120 mm	1200 W	80"/min

Material: 304L Stainless Steel
Heat : 481361 (1.92 Cr/Ni)
Laser: Rofin Nd:YAG

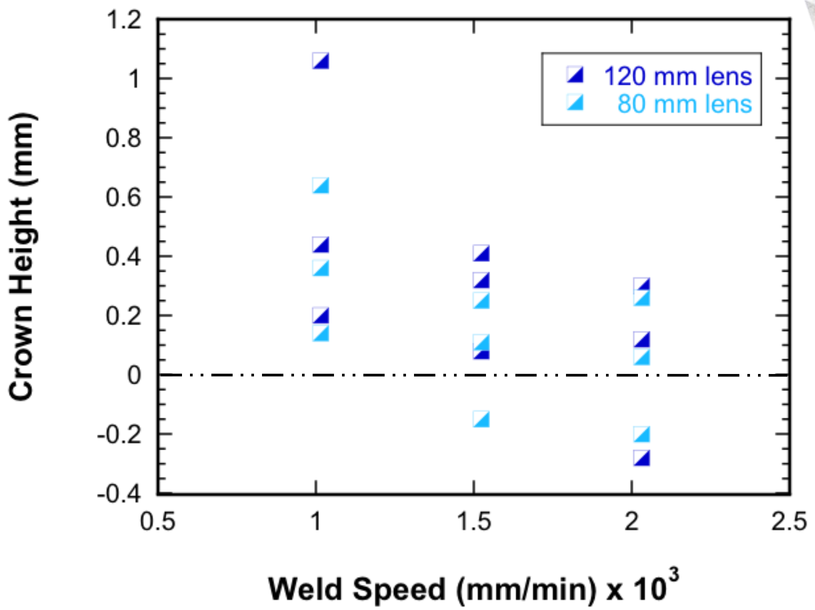

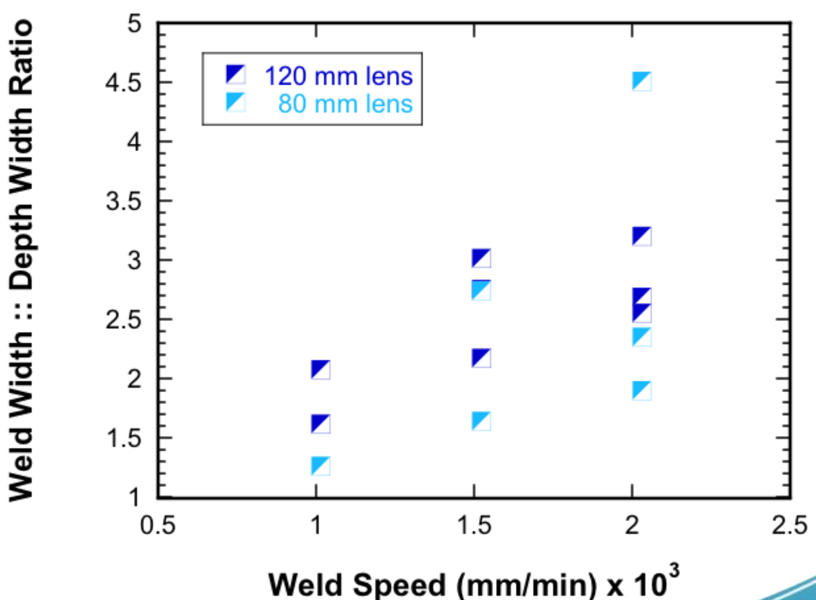

µ-Computed Tomography

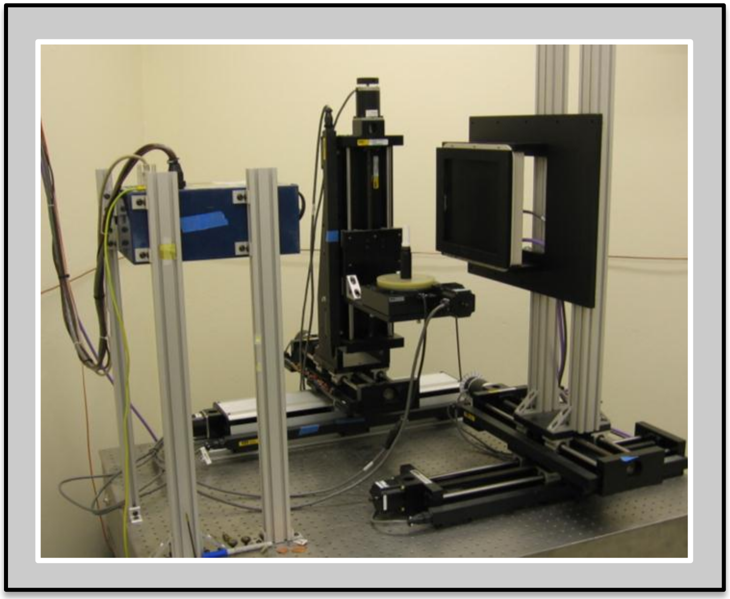

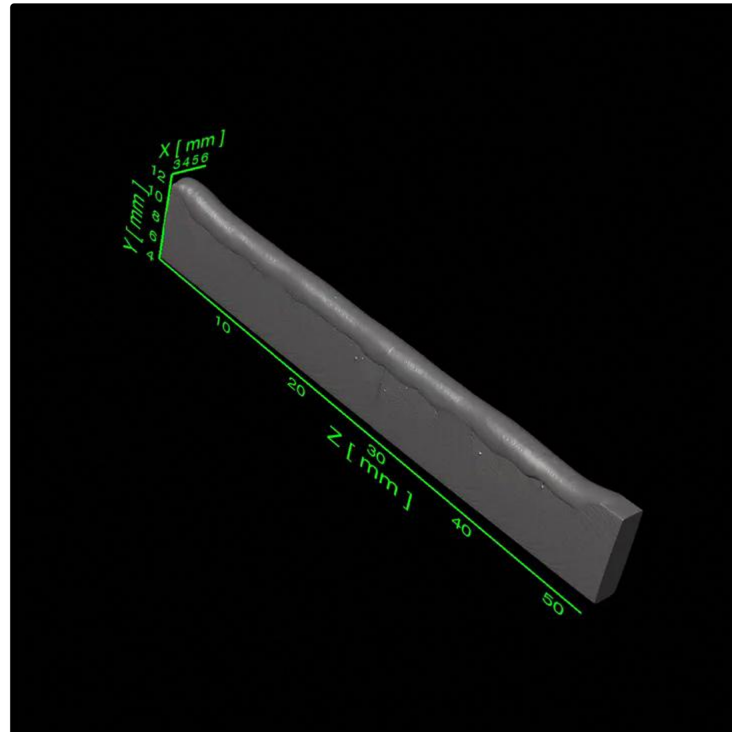

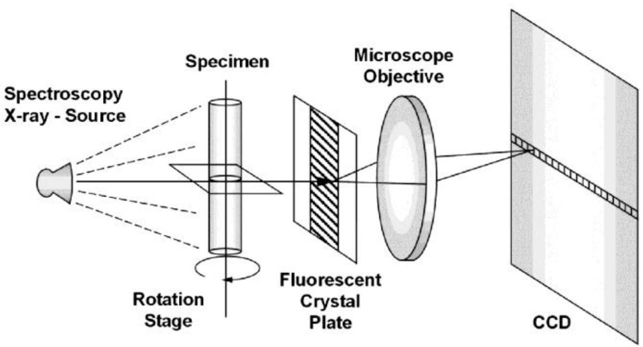

M.D. Bentley, et al. *Am. J. Physiol. Regul. Integr. Comp. Physiol.*,vol. 282, no. 5 (2002)

- Rotation occurs counter clock-wise in front of a fluorescent cesium iodide plate
- 9X magnification yields an effective pixel size of 14 um
- Energy is set to 130KV and 250uA yielding a spot size on the order of 27 um
- Objects 14 um in size can be detected but resolution is not adequate until objects reach 27 um in size

Quantifying Porosity

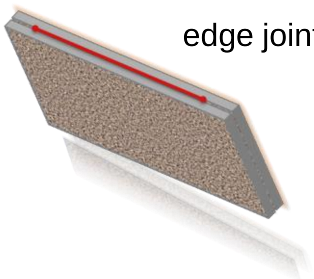

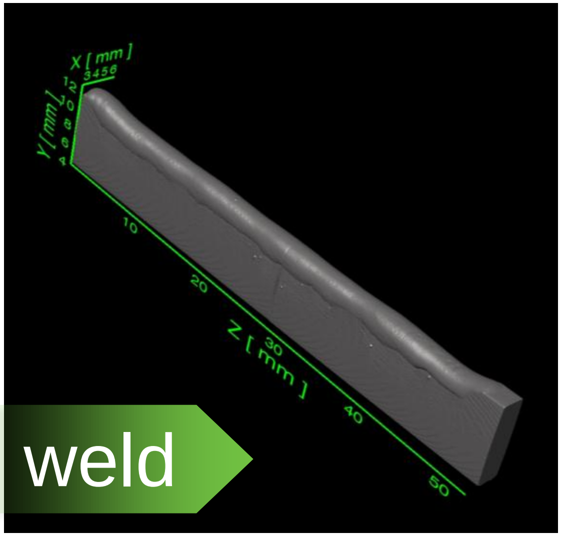

weld

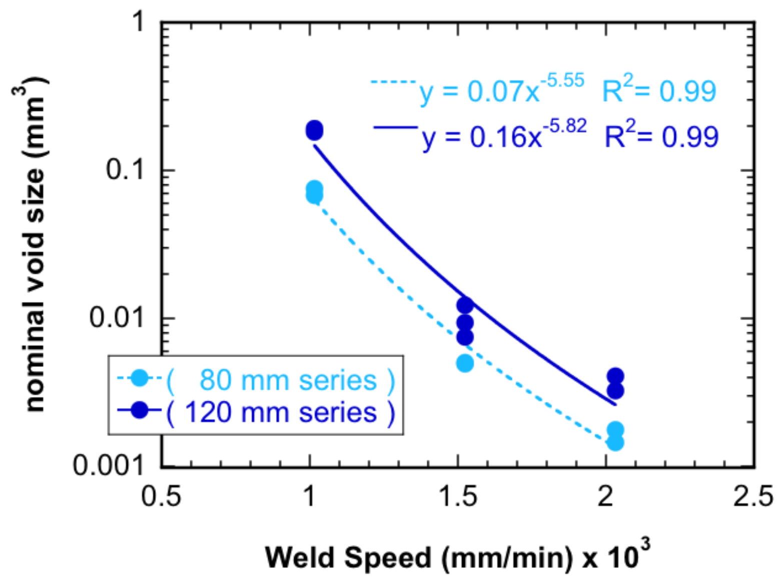

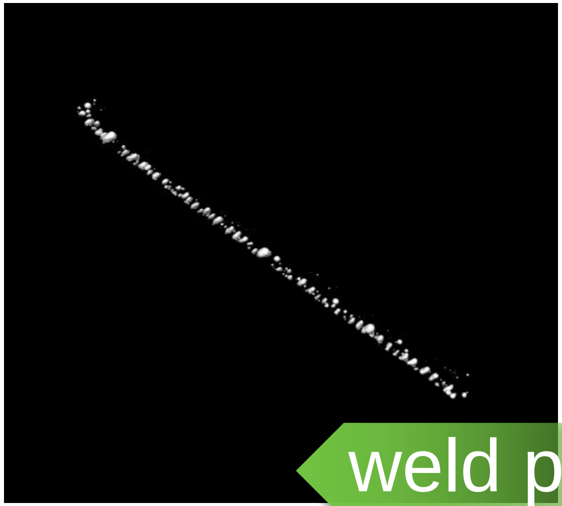

weld porosity

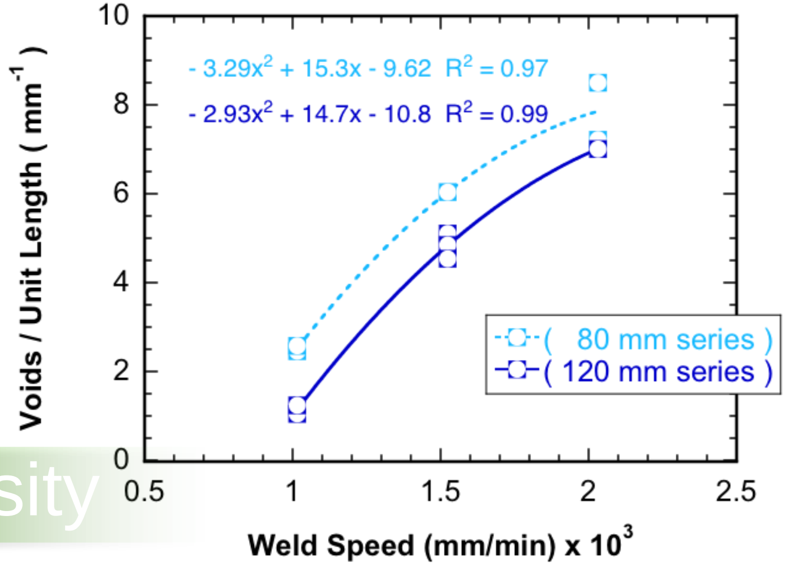

Porosity Volume Fraction

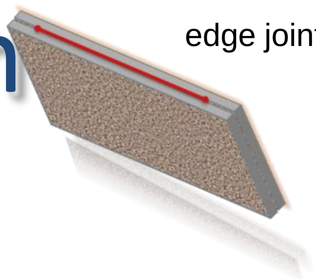

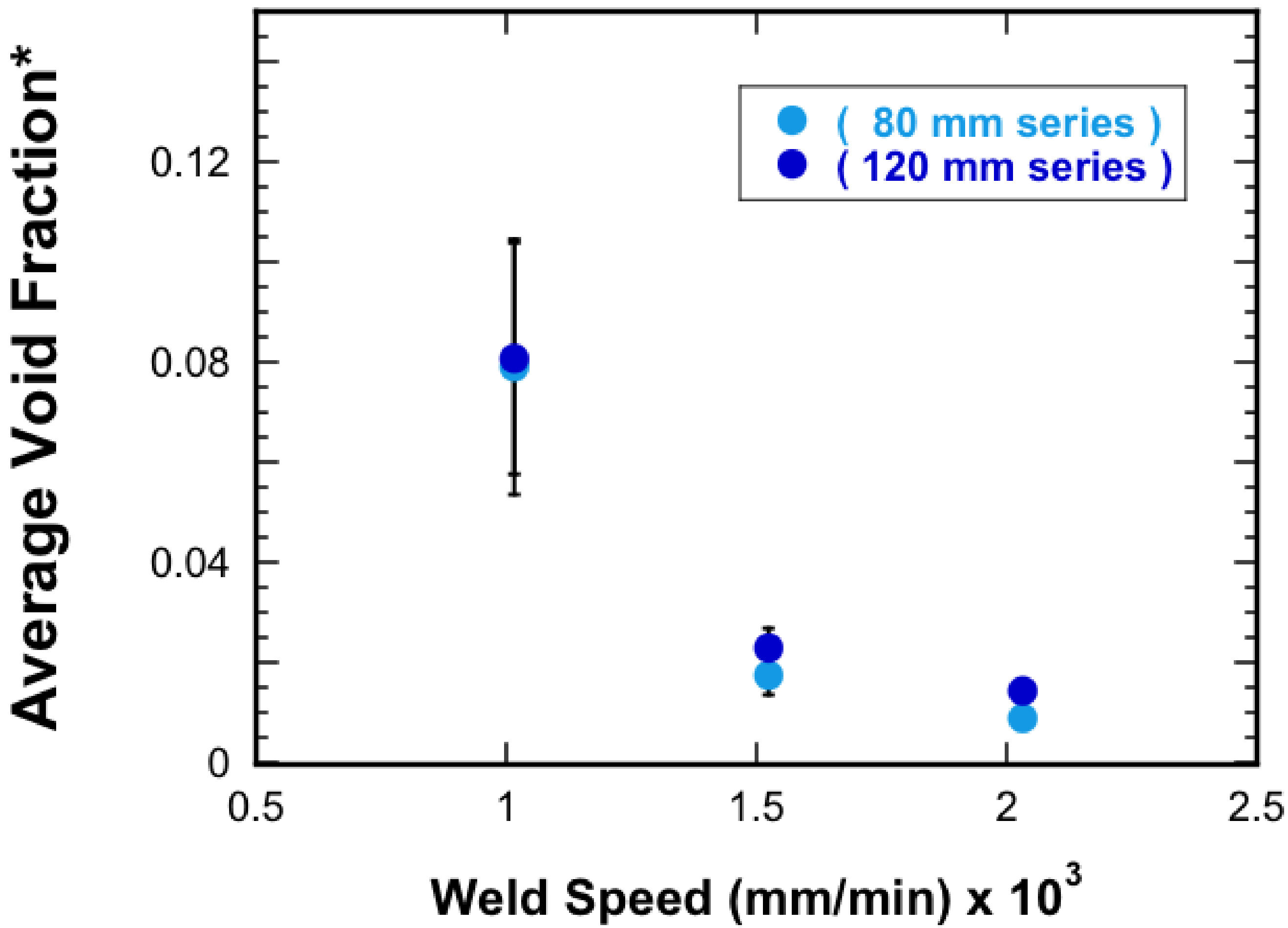

* Uncertainty is derived from measuring weld volume precisely, not porosity amounts

Quantifying Porosity

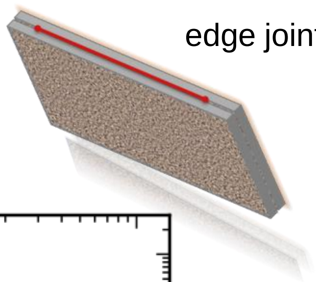

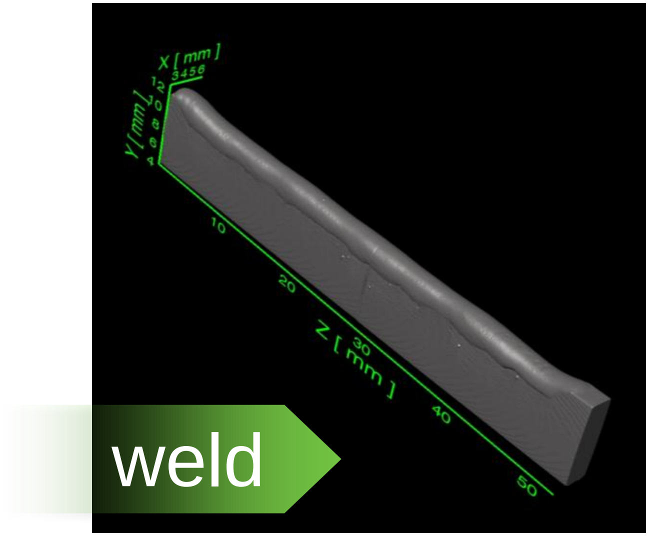

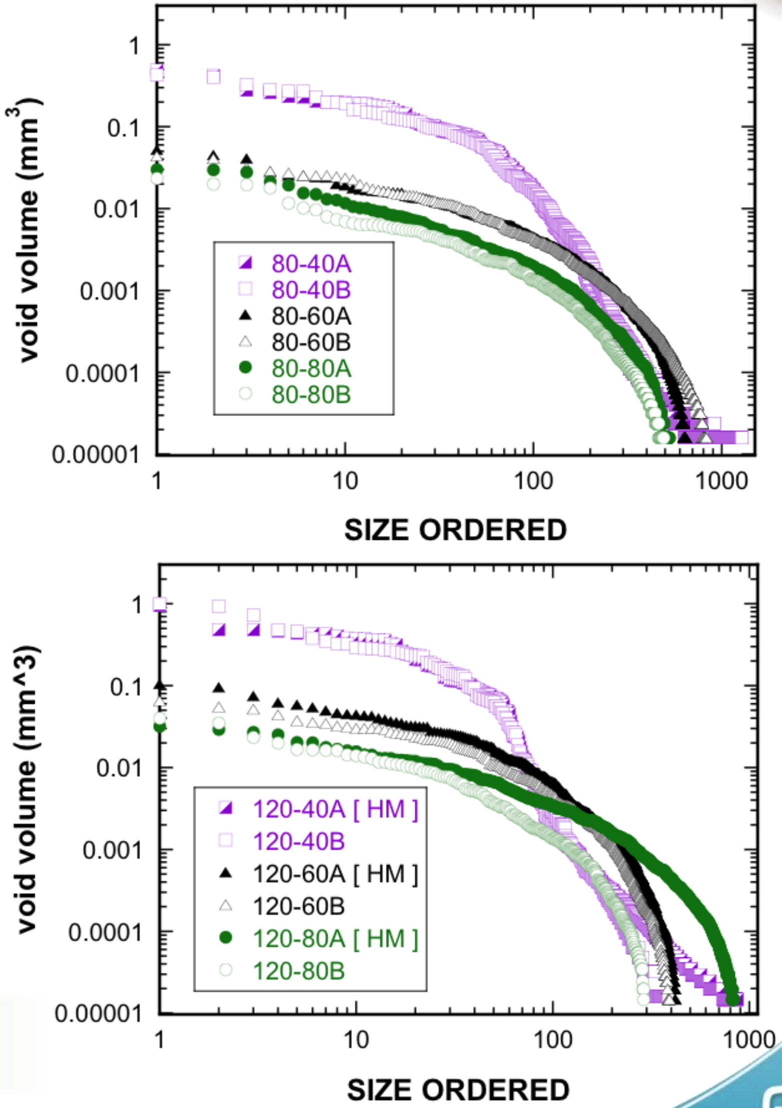

Porosity Distributions

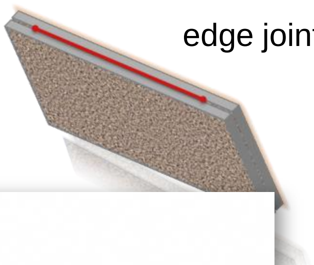

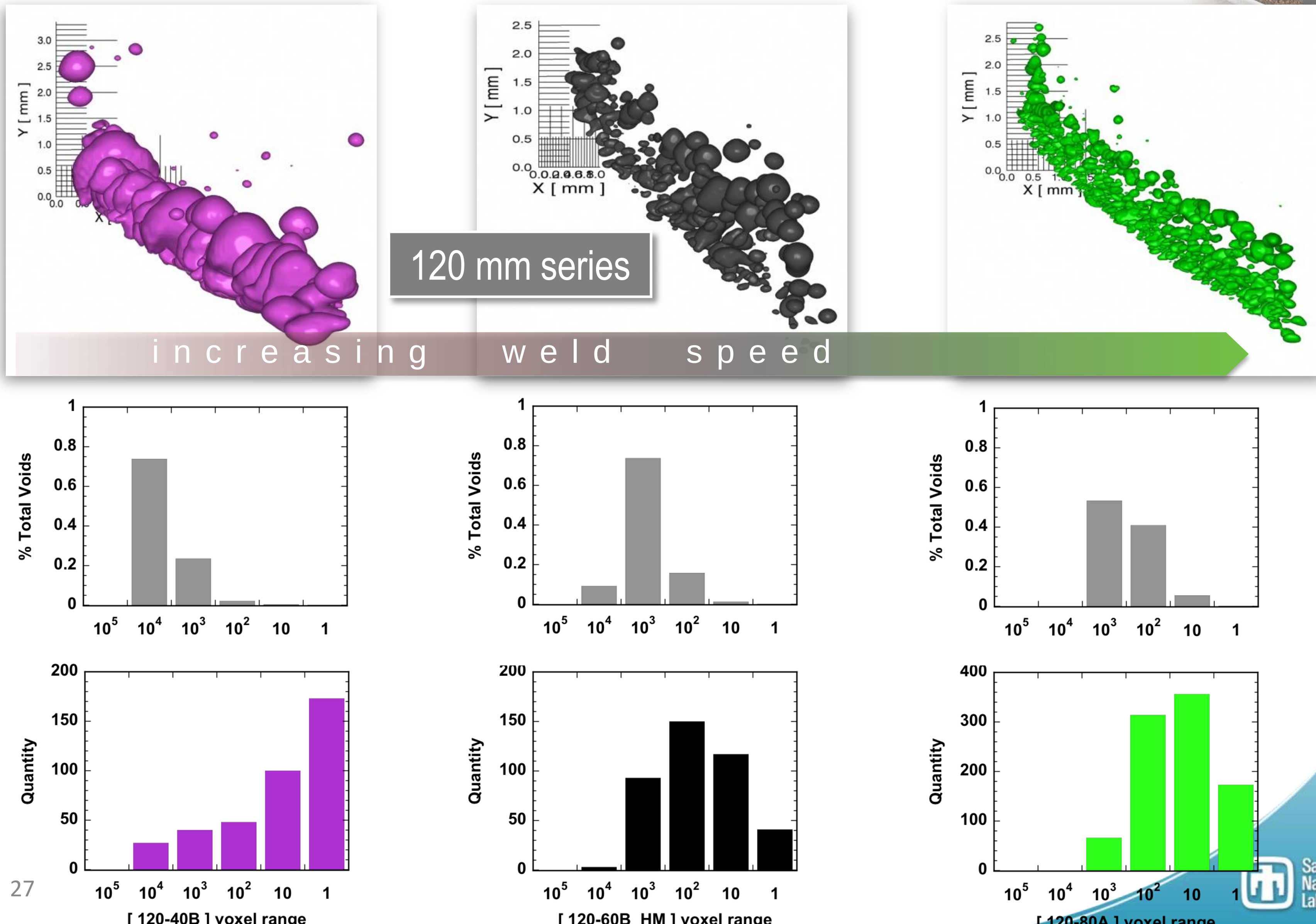

Sandia National Laboratories

Porosity Morphology

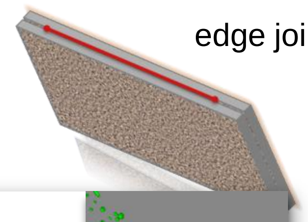

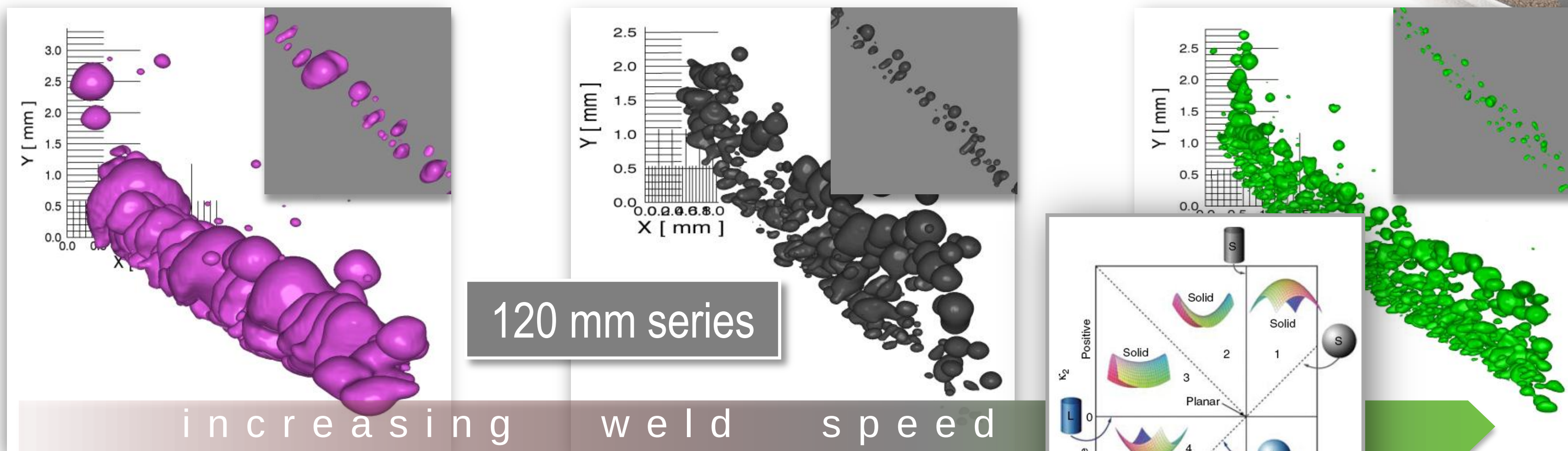

Mendoza, Alkemper & Voorhees, The Morphological Evolution of Dendritic Microstructures During Coarsening, ***Met Trans A,*** *Vol. 34A (2003) pp. 481-489*

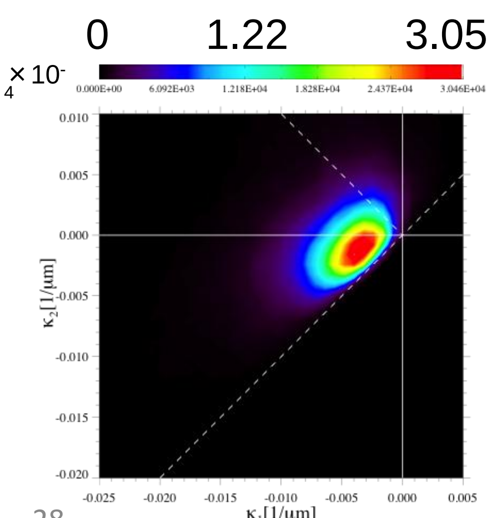

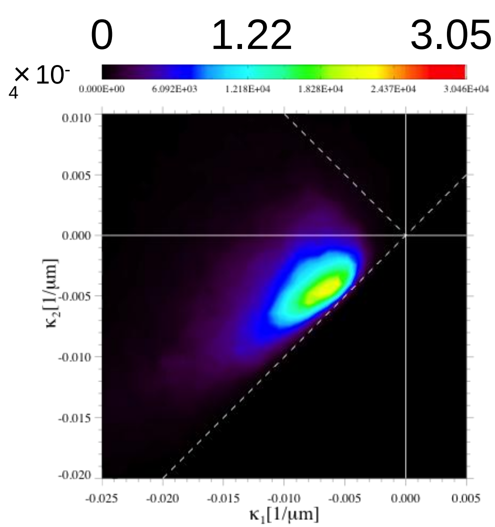

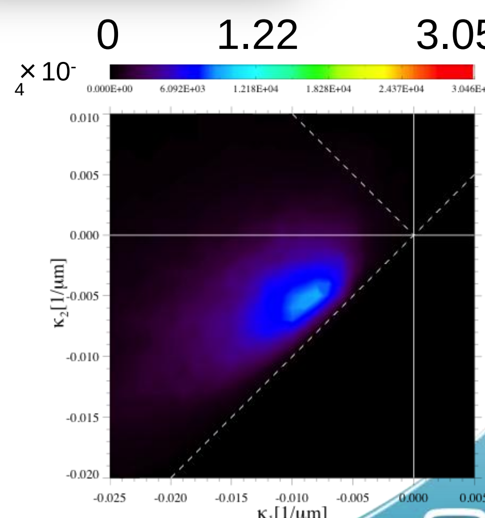

Sandia National Laboratories

Porosity Distributions

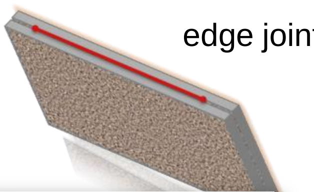

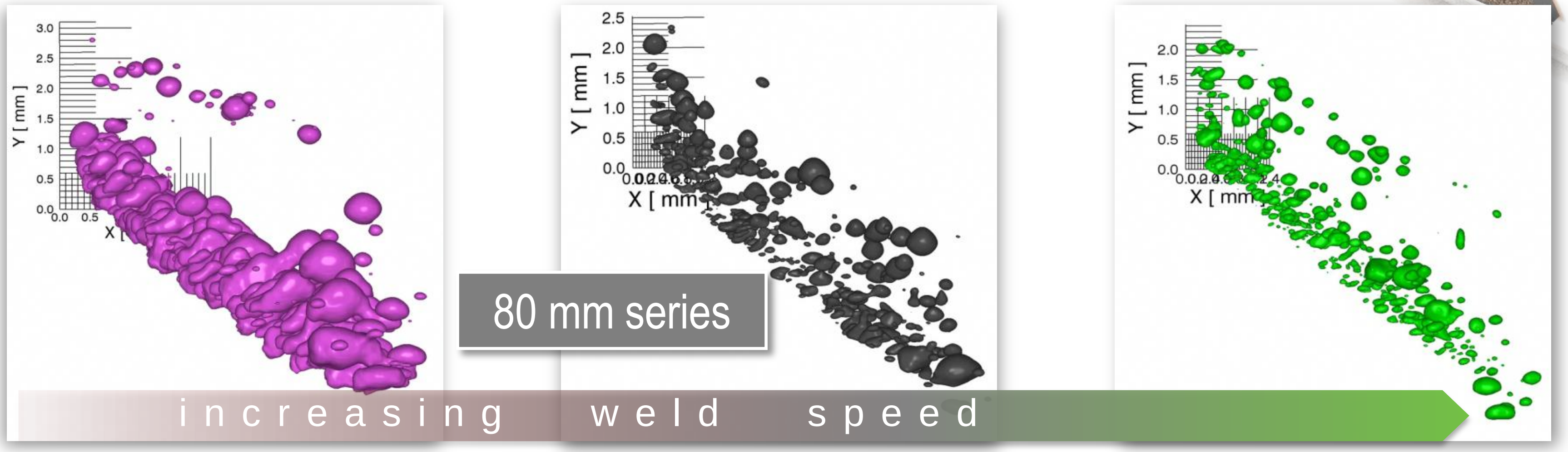

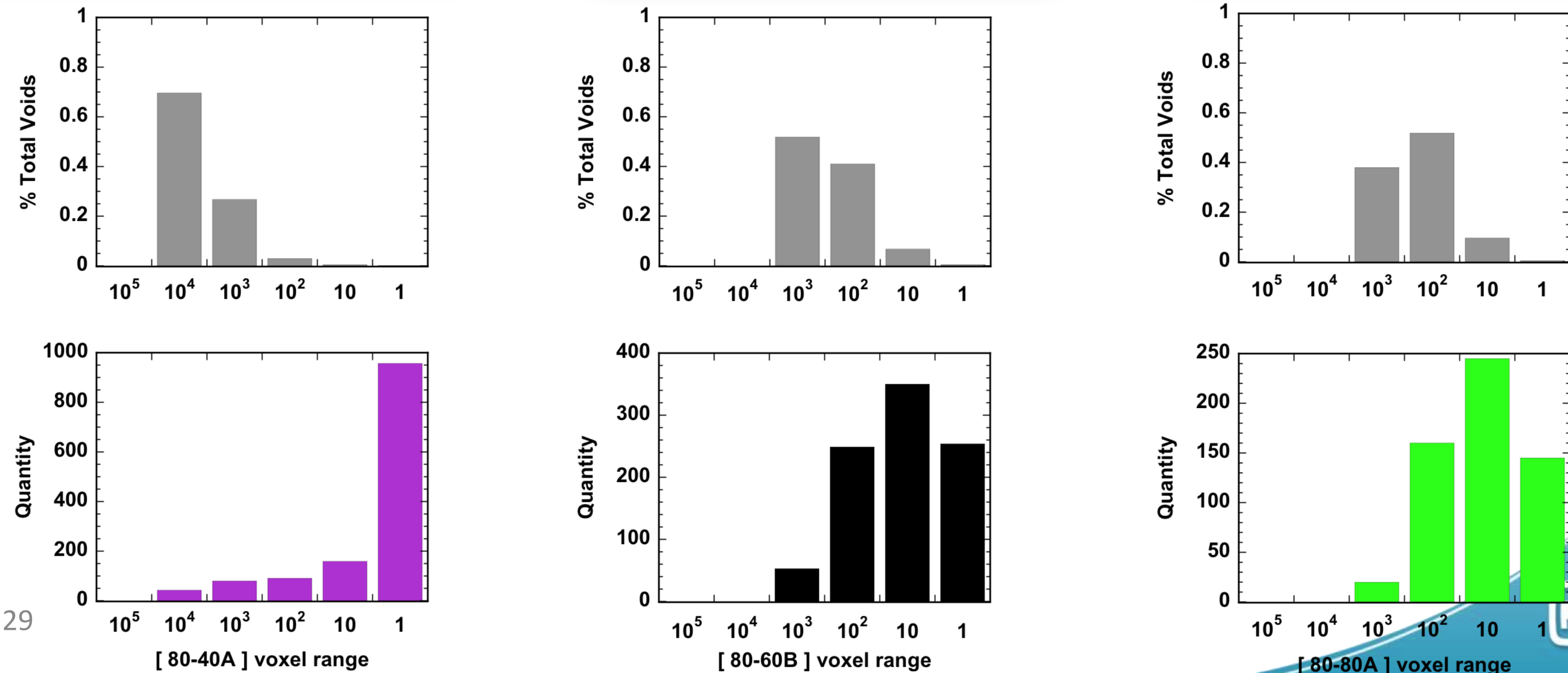

Porosity Morphology

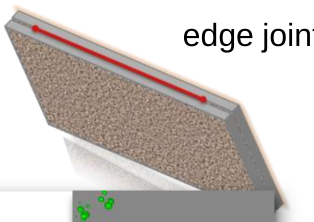

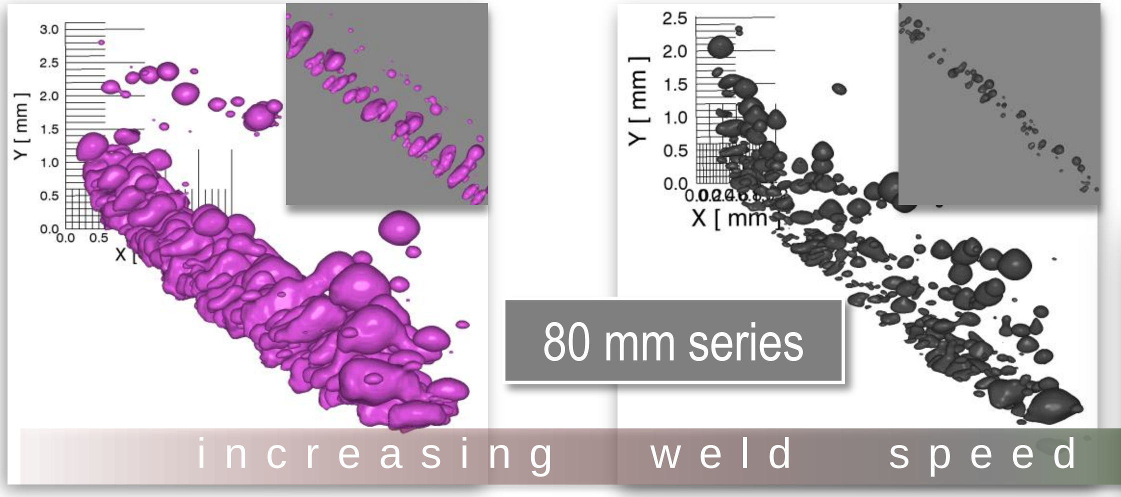

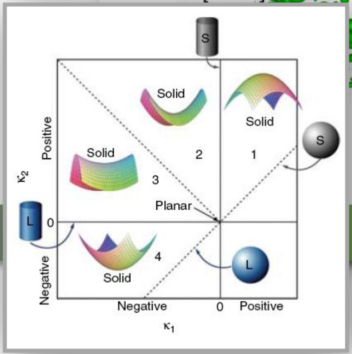

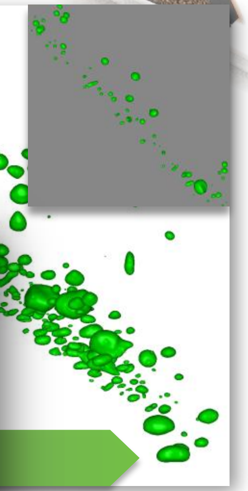

Mendoza, Alkemper & Voorhees, The Morphological Evolution of Dendritic Microstructures During Coarsening, ***Met Trans A,*** *Vol. 34A (2003) pp. 481-489*

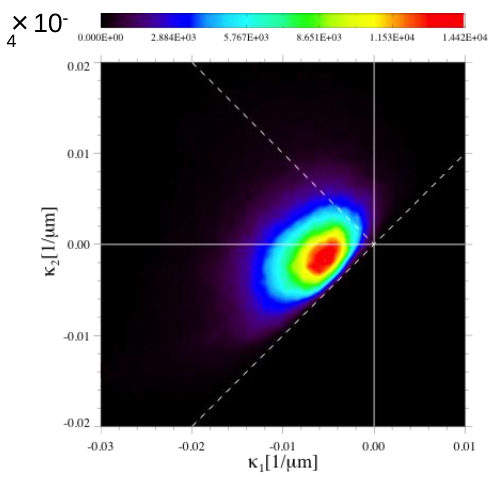

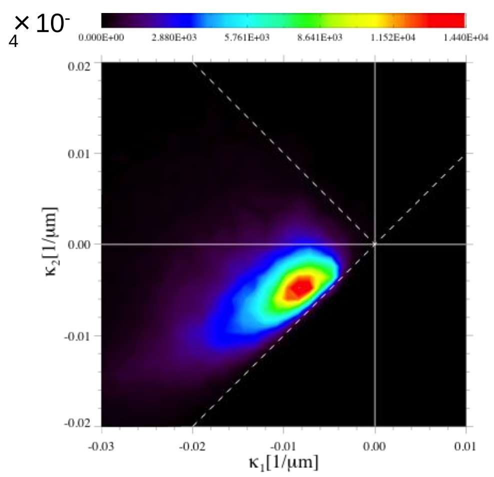

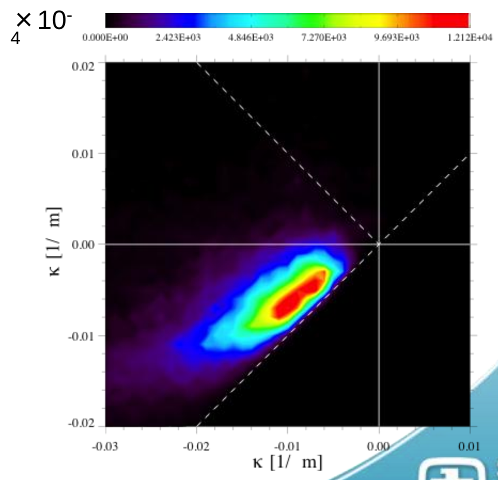

Sandia National Laboratories

Shape Anisotropy

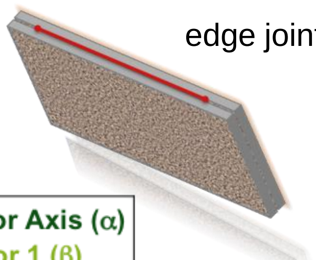

edge joint

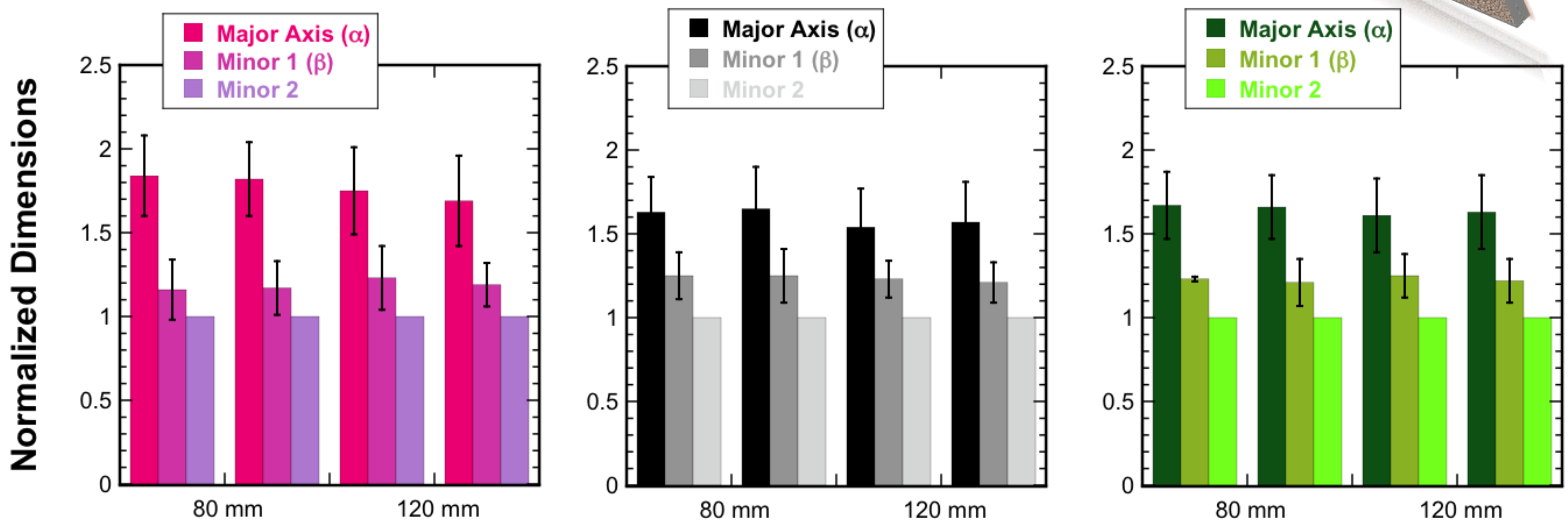

1016 mm/min

$\alpha = 1.69 - 1.85$
$\beta = 1.19 - 1.23$

1524 mm/min

$\alpha = 1.54 - 1.65$
$\beta = 1.21 - 1.25$

2032 mm/min

$\alpha = 1.61 - 1.67$
$\beta = 1.21 - 1.25$

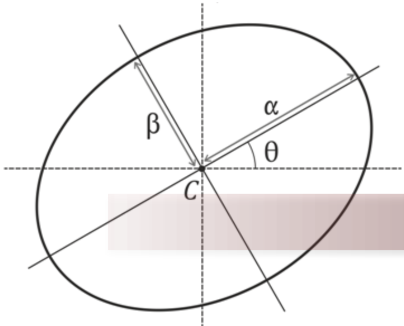

i n c r e a s i n g   w e l d   s p e e d

Sandia National Laboratories

Directional Anisotropy

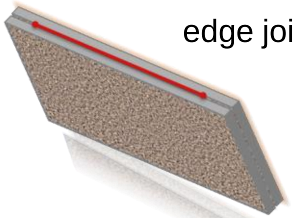

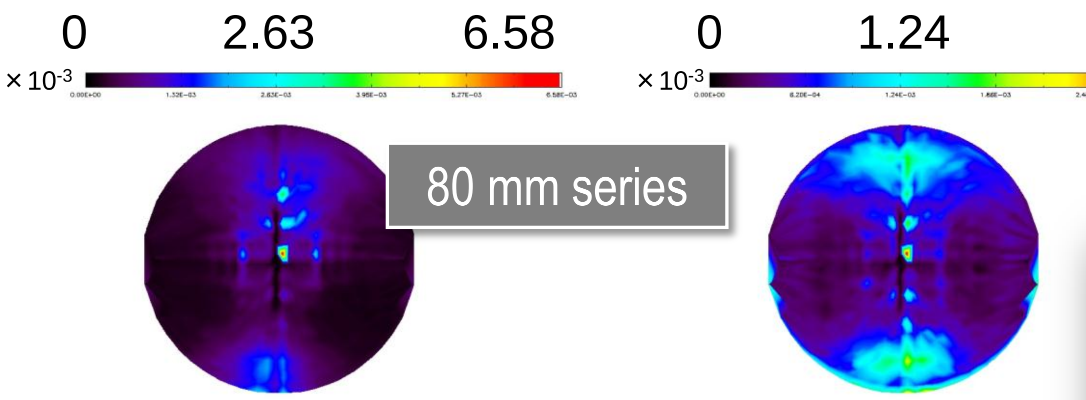

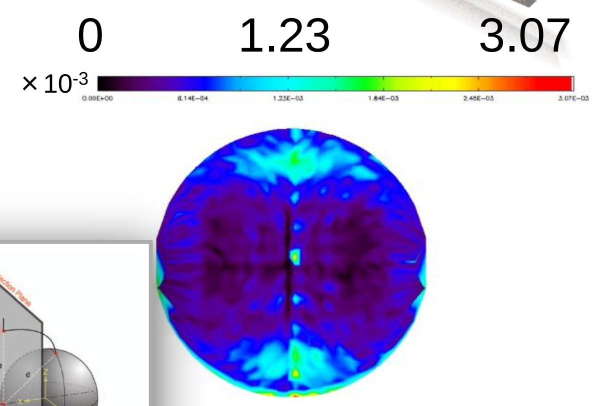

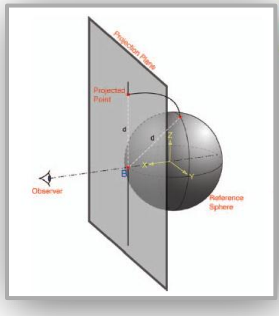

*Kammer & Voorhees, The Morphological Evolution of Dendritic Microstructures During Coarsening, **Acta Mater.,** 54, (2006) pp. 1549-1558*

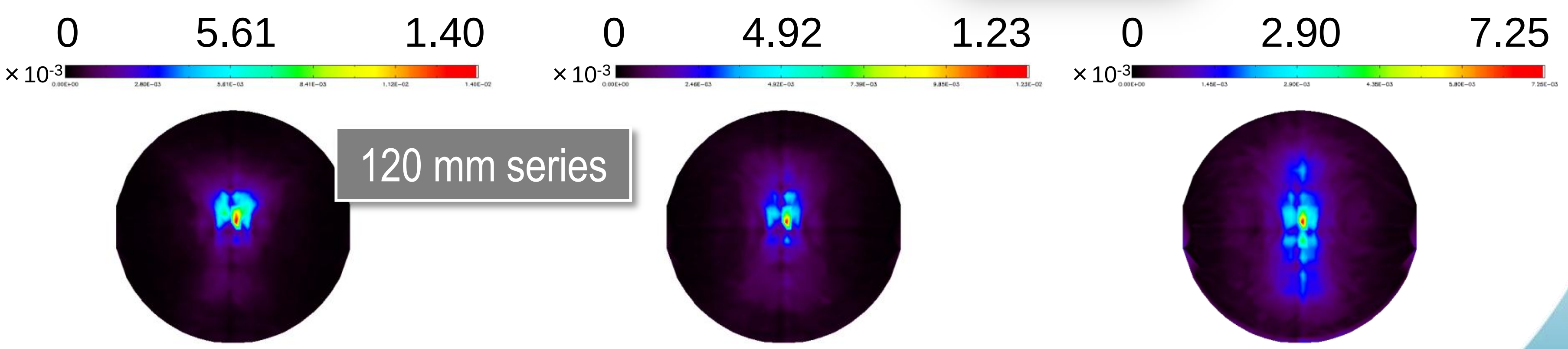

Modeling Approach

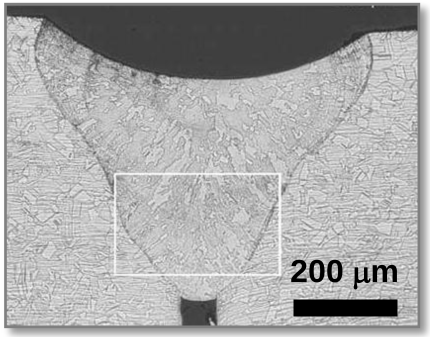

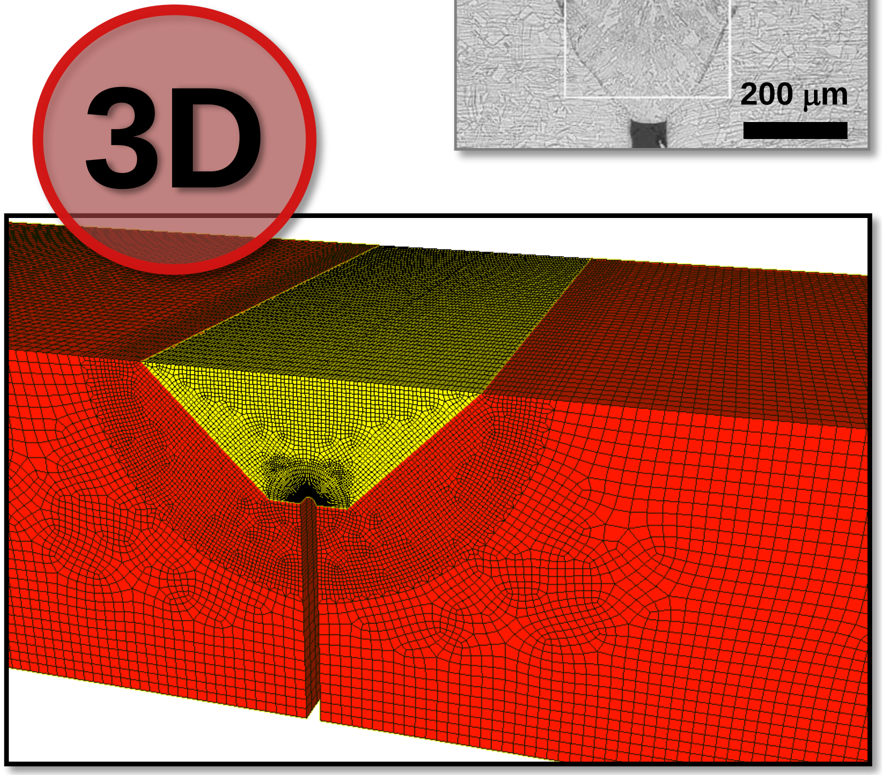

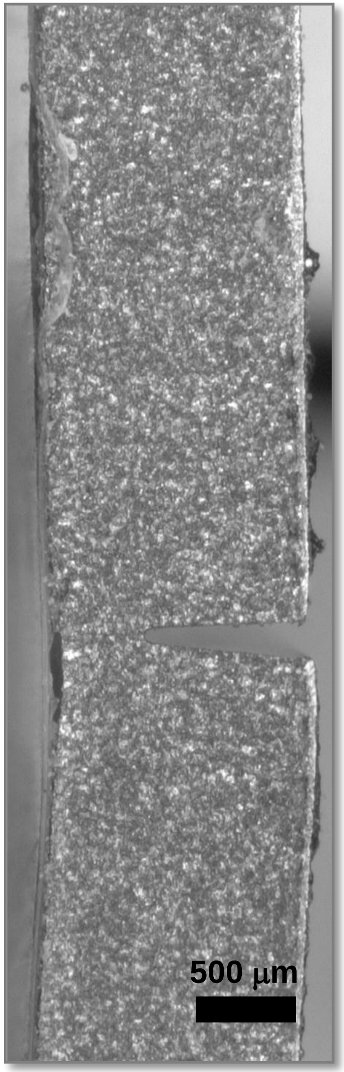

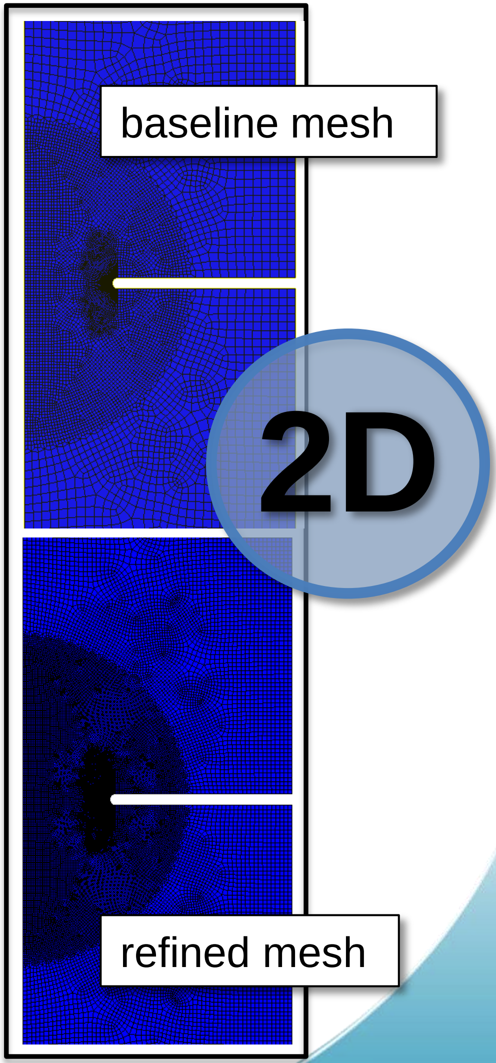

Initial models are vastly simplified. We only seek to understand general trends.

Simulation Trends (2D)

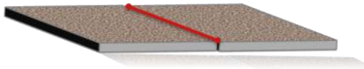

butt joint

Rather than model an effective media, we attempt to model individual pores and initially take the matrix to be the bound for the weld material. To facilitate our understanding, we begin with 2-D plane strain.

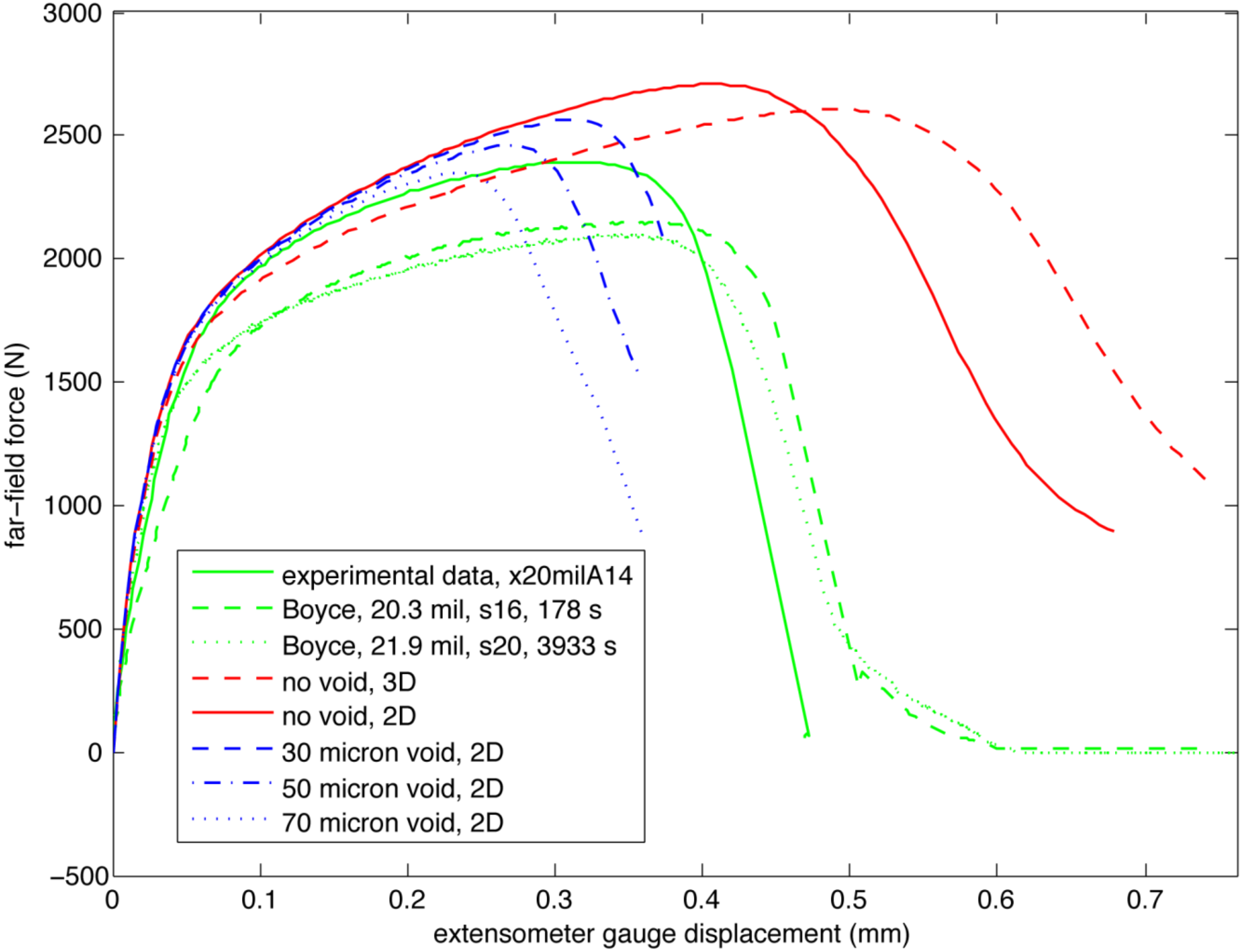

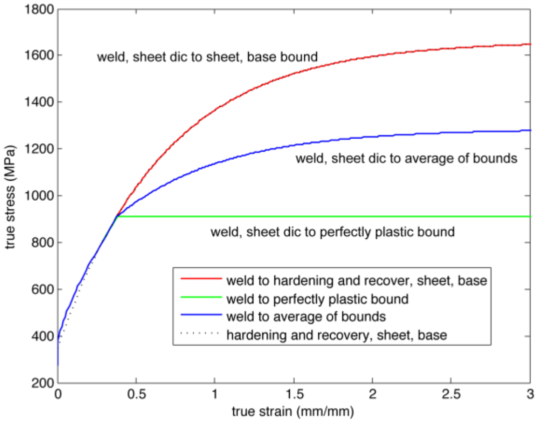

weld, sheet dic to sheet, base bound

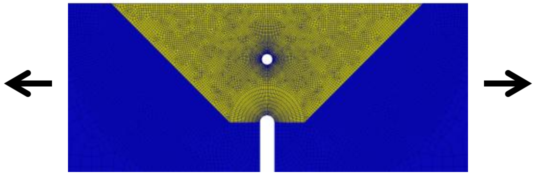

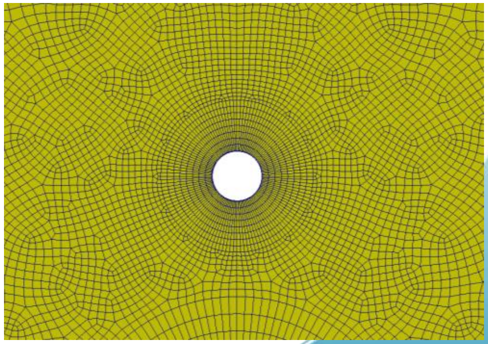

50 μm pore centered in ligament

Sandia National Laboratories

Void Interaction and Necking (2D)

The peak load is heavily influenced by the void interaction with the notch and the free surface

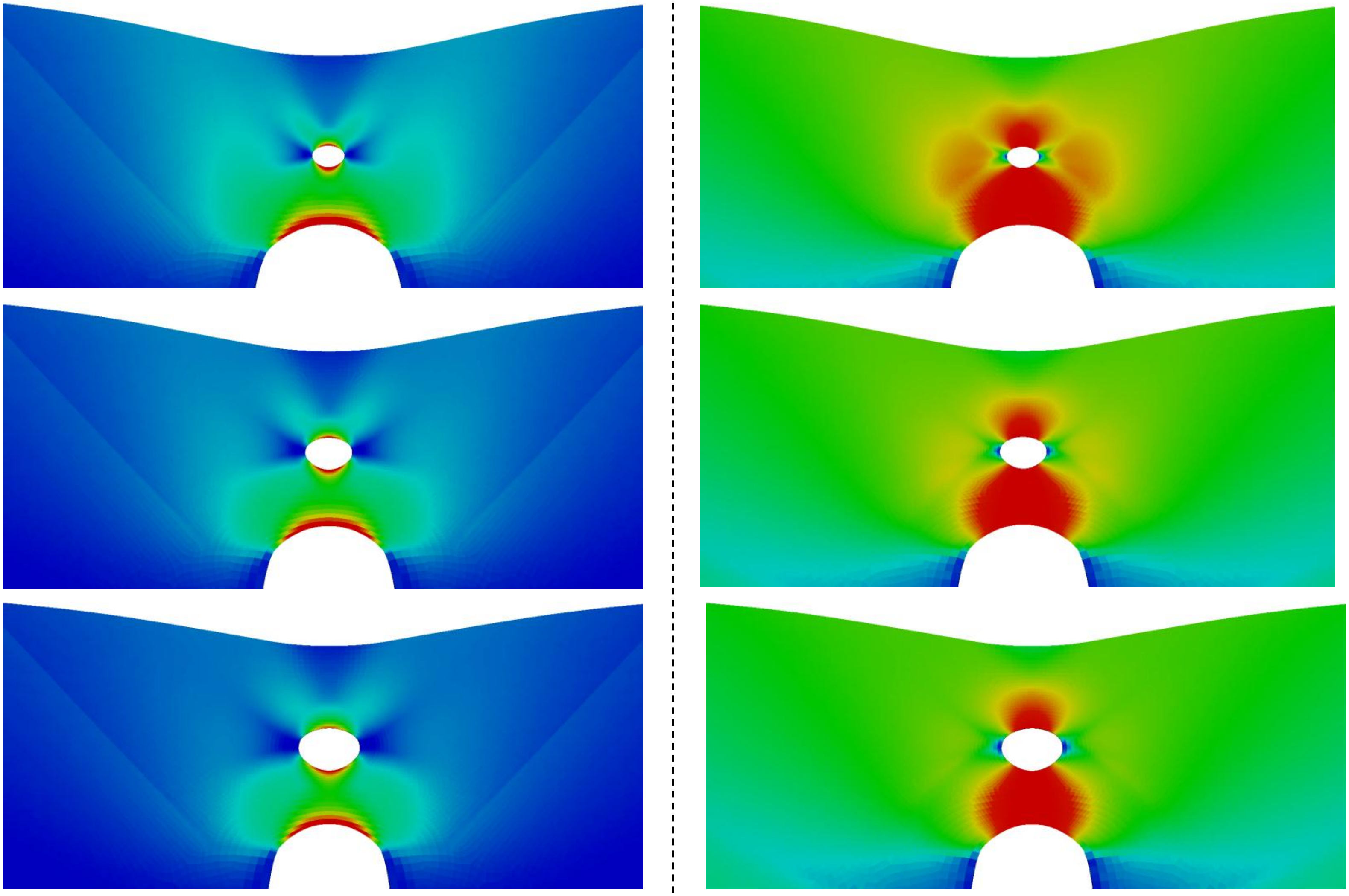

30 μm pore
P_{max} = 2570 N
Δ = 0.314 mm

50 μm pore
P_{max} = 2460 N
Δ = 0.270 mm

70 μm pore
P_{max} = 2350 N
Δ = 0.236 mm

$0 < \varepsilon_p < 1$

$0 < \sigma_{axial} < 1.5\ GPa$

Simulations of Yield (3D)

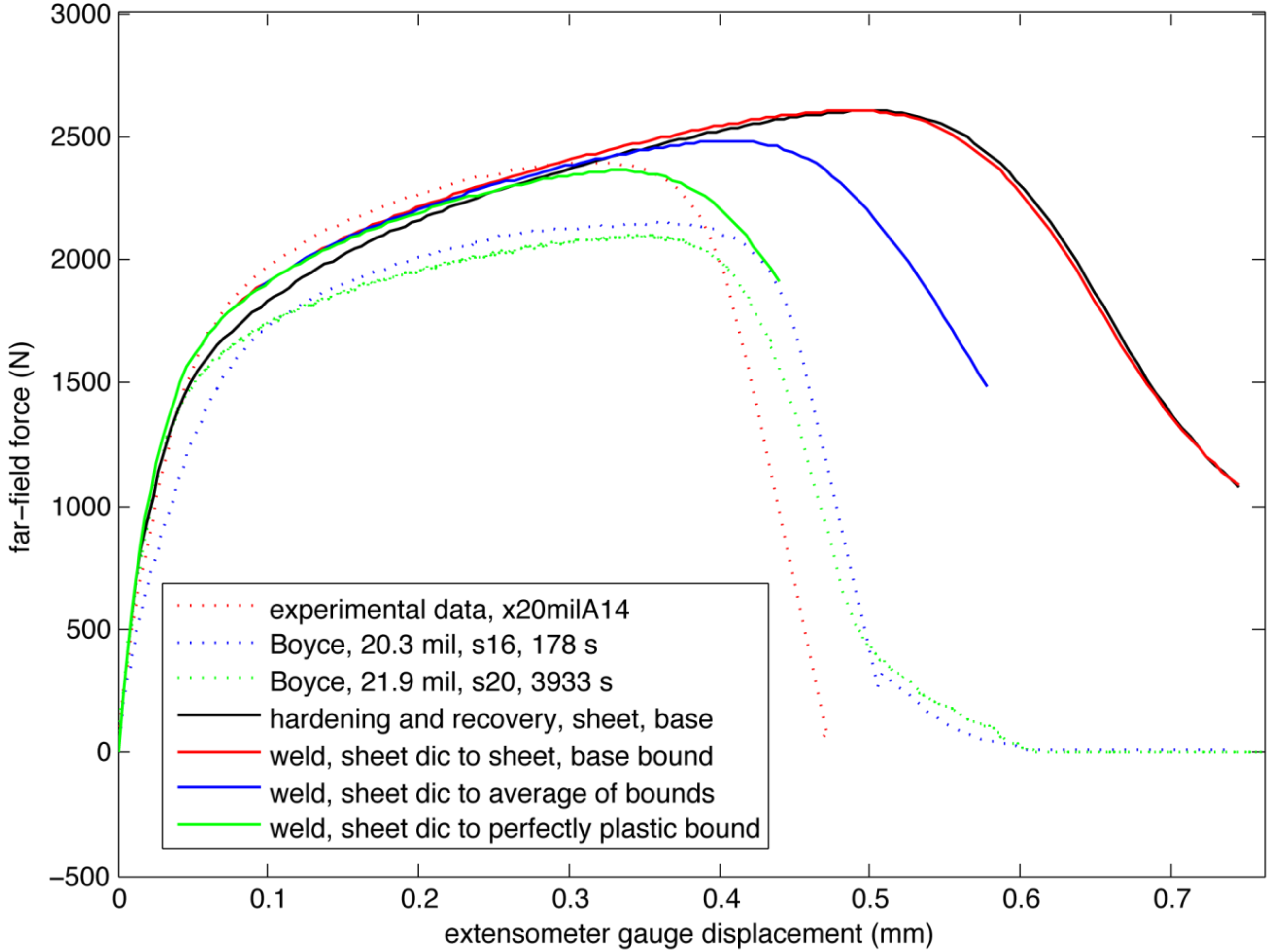

We must assume perfect plasticity to correlate with experimental findings.

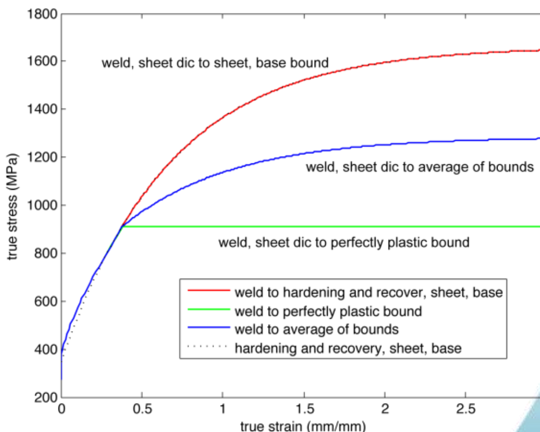

These limited findings illustrate the need for including more than plasticity. Limited softening from porosity evolution might explain both tensile and weld configurations. More work is needed.

Sandia National Laboratories

Fields for Perfect Plasticity (3D)

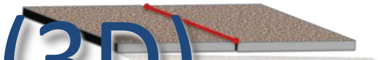
butt joint

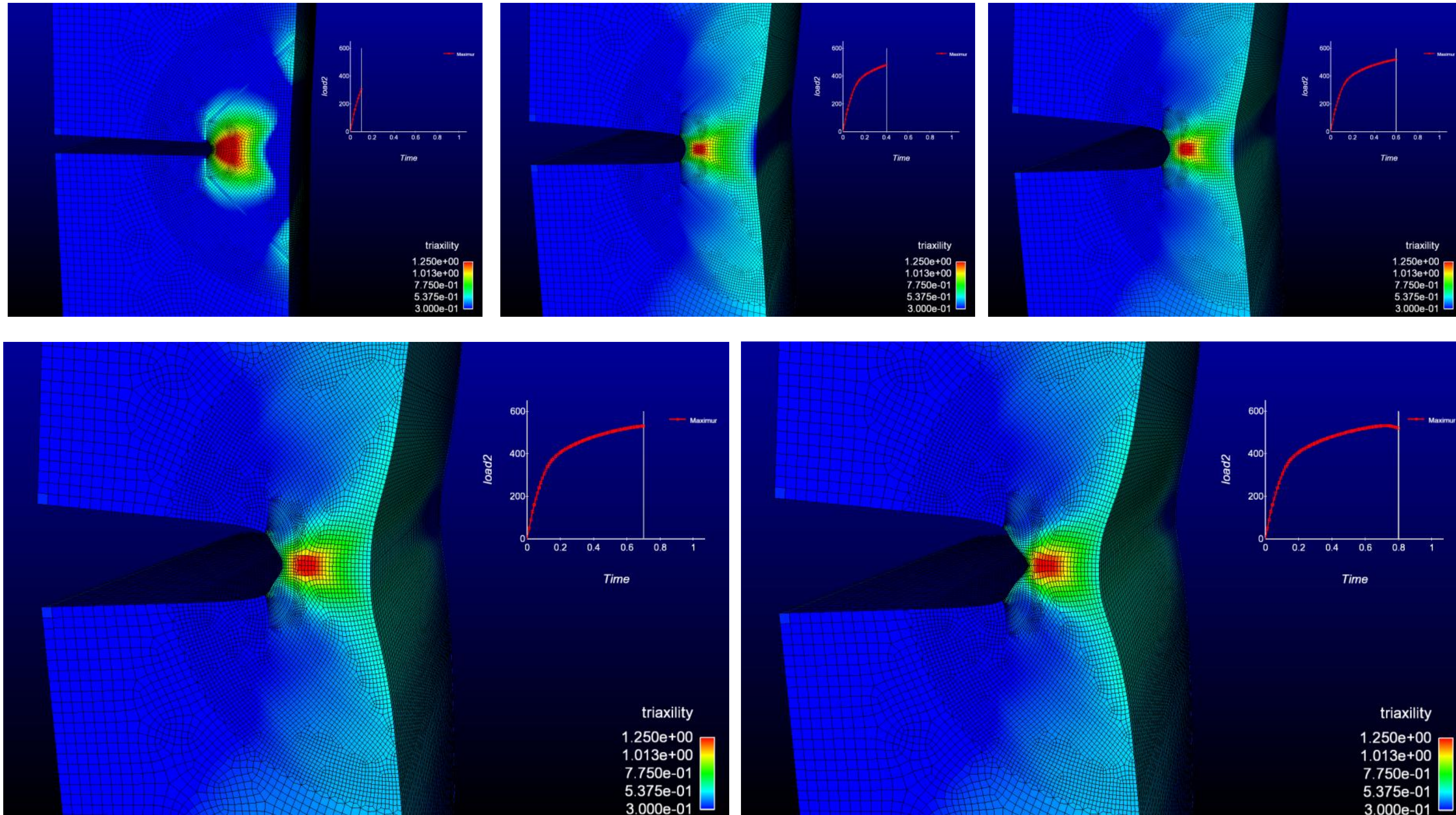

The triaxility is elevated throughout the entire deformation process. Void growth need not be limited to the secondary necking response.

Summary

- [µCT] provides a relatively rapid means to gain 3d evaluations of millimeter scale weld porosity down to a resolution of 27 μm^3
- In larger welds, across all welds examined, the most frequently occurring void sizes constitute less than 10% of the total porosity found
- We can now measure subtle changes in average and specific measures of porosity in millimeter scale welds *(i.e. porosity size, amount/length, volume fraction, size distributions)* in welds and relate them to changes in processing parameters
- We have been able to effectively quantify changes in porosity shape as well as directionality which may present useful inputs for modeling mechanical response in welds of this size and character

Part II

Simulation of Dynamic Recrystallization in Uranium Dioxide Nuclear Fuels

Outline

- Background
  - Nuclear Fuels
  - High Burn Up Structure
- Simulation Framework
- Algorithm Components
  - Grain Growth via kMC
  - Recrystallization via CA
  - Energy Accumulation & Nucleation
- Results
  - Effects on System Energy & Grain Size
  - Hybrid Algorithm
  - Representative Volume
- Future Work
- Conclusions

Nuclear Fuels

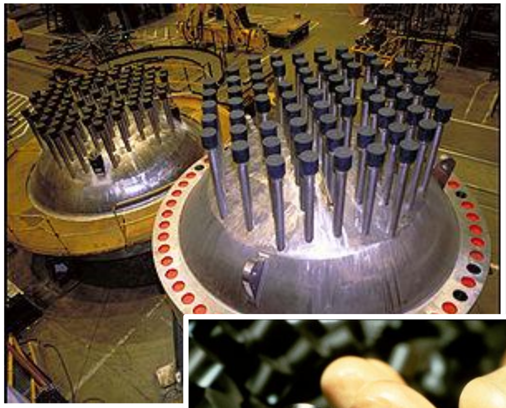

Pressurized Water Reactor
www.nrc.gov

Nuclear Fuel Pellet
www.nrc.gov

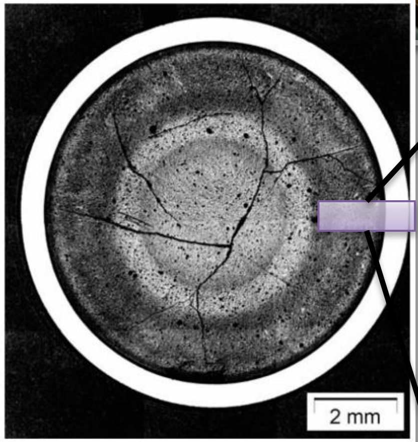

Irradiated Fuel Cross-Section
Noirot, et. al ***NE&T****, vol. 41 2009*

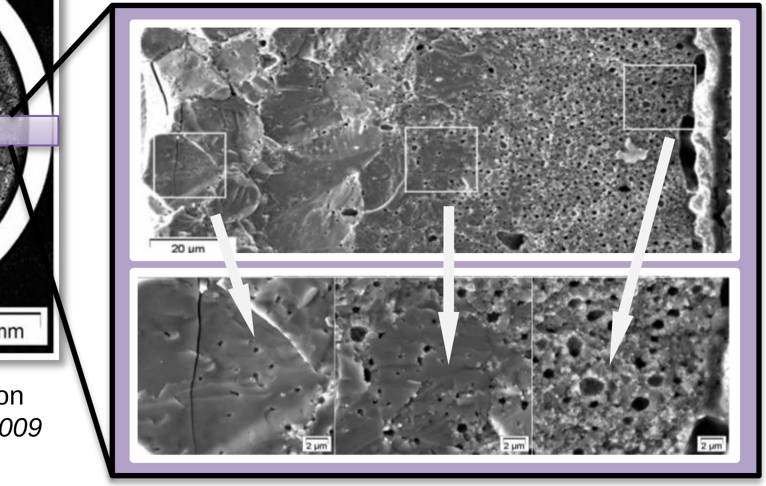

- **The rim of LWR fuels is enriched relative to the rest of the fuel by resonance neutrons which are preferentially absorbed by ^{238}U at the surface.**
- **$^{238}U + n \rightarrow {}^{239}U \rightarrow {}^{239}Np + \beta^- \rightarrow {}^{239}Pu + \beta^-$**
- **Enrichment of fissile material in the rim, resulting in more fission events**
- **Damage accumulates follows fission rate**
- **Relatively low temperature causing repeated recrystallization**

RESULT

Tremendous Variation In Microstructure

1. Grain size
2. Porosity
3. Percolation
3. Composition
4. Hardness

High Burn-Up Structure I

- Rim structure is a function of burn-up
- Low burn-up, original grain structure
- With ^{239}Pu formation, recrystallization occurs where enrichment is most pronounced

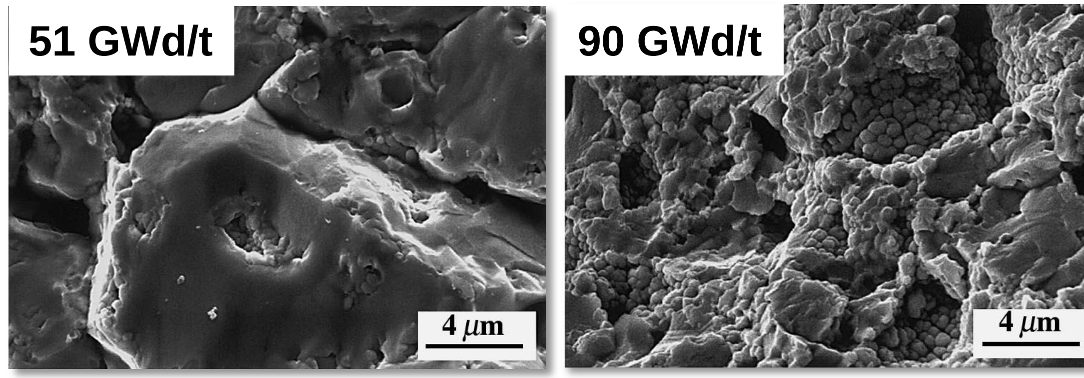

*Une, et. al, **JNM** vol. 288, 2001*

- Since burn-up correlates with radial position recrystallization is largely absent as r/r_o decreases

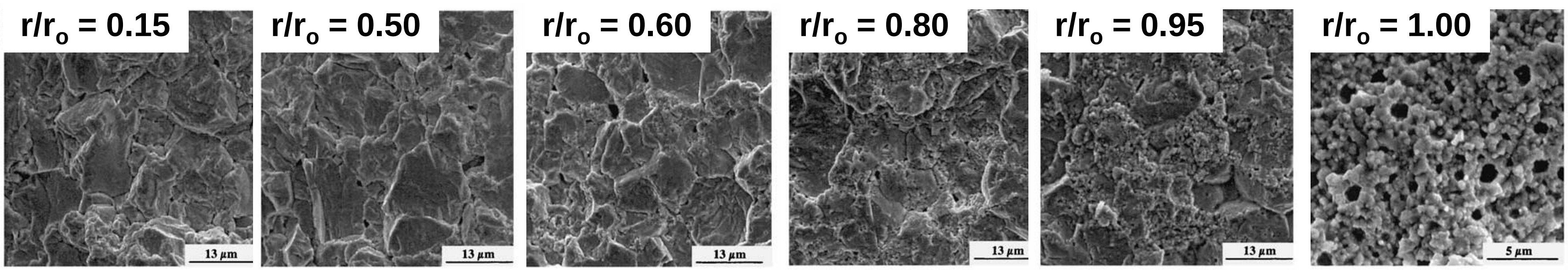

*Manzel & Walker, **JNM** vol. 301, 2002*

High Burn-Up Structure II

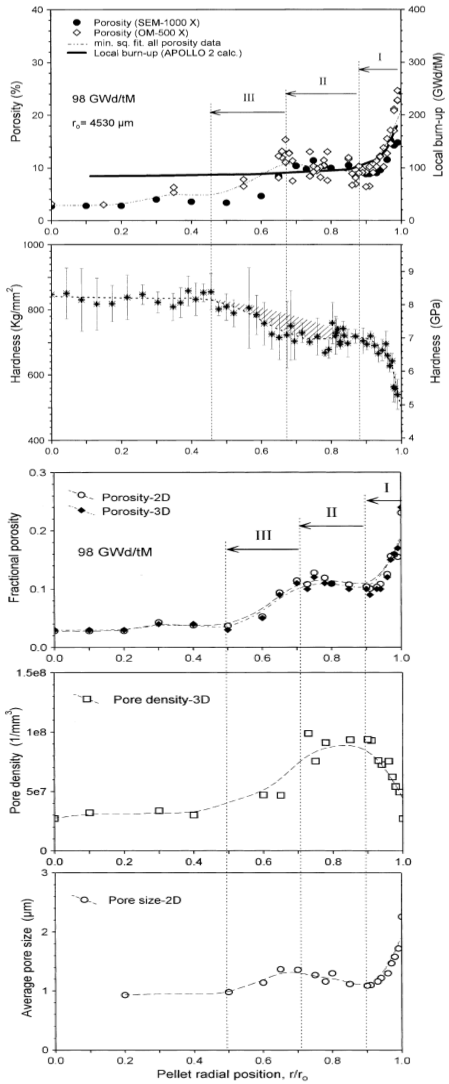

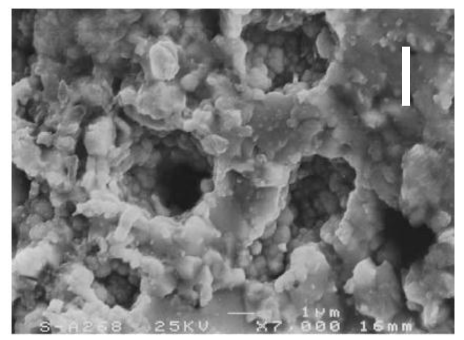

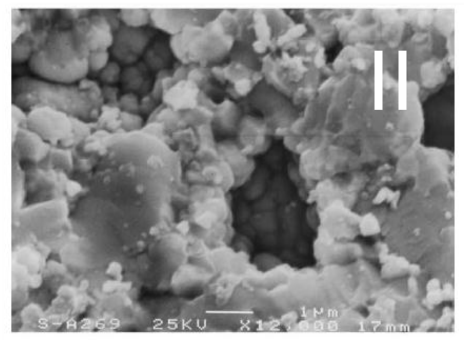

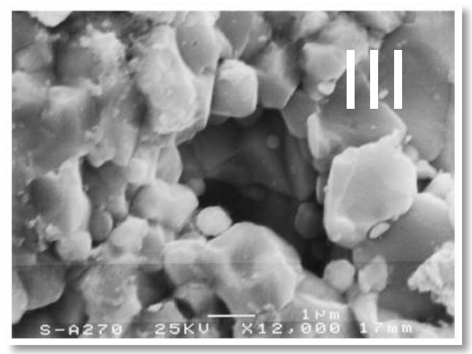

- Understanding the rim effect is important
  - Effects fuel performance (thermal conductivity, fission product distributions, …)
  - Effects mechanical properties during storage and transportation
  - Modifies the separation processes for fuel recycling.

- Various aspects of the evolutionary process are analagous to metallic systems undergoing dynamic recrystallization.

Spino et al., ***JNM*** *vol. 354, 2006*

Simulation Framework

SPPARKS

Kinetic Monte Carlo via Stochastic Parallel PARticle Kinetic Simulator

- Development a new user application for SNL's SPPARKS open-source environment
- Treat grain growth + dynamic recrystallization events simultaneously
- Incorporate probabilistic cellular-automaton approach to more accurately capture realistic kinetics (KJMA rates)
- Toward prediction of microstructural evolution in irradiated materials beyond currently established NRC regulations

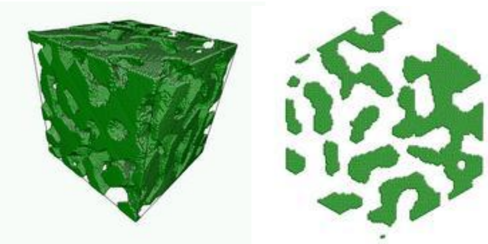

Wagner

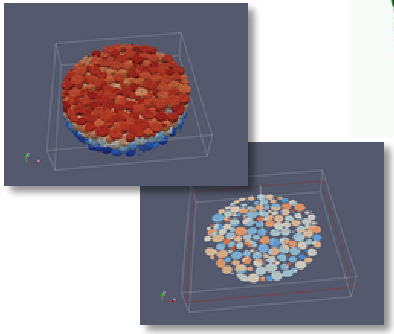

Tikare & Garcia-Cardona

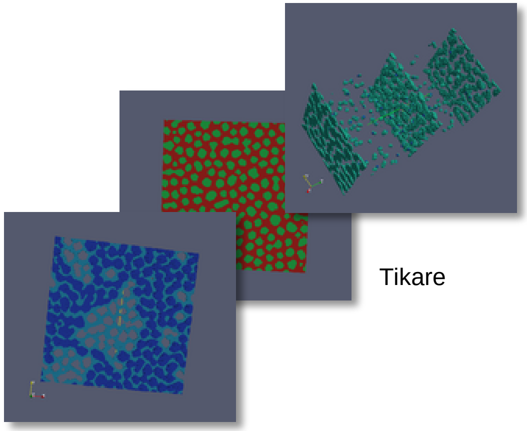

Tikare

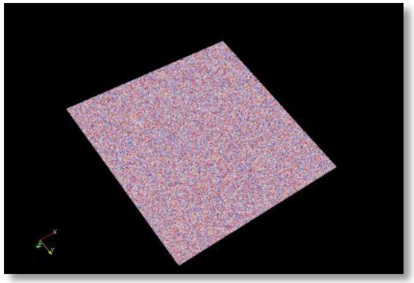

Sandia National Laboratories

http://www.cs.sandia.gov/~sjplimp/spparks.html

Algorithm Components

Kinetic Monte Carlo

+

Cellular Automata

Stochastic, probability driven evolution

C.C. Battaile, The Kinetic Monte Carlo Method: Foundation, Implementation, and Application, Computer Methods in Applied Mechanics and Engineering, 197 (2008) 3386-3398.
H. Barreto, F.M. Howland, Introductory Econometrics: Using Monte Carlo Simulation with Microsoft Excel, Cambridge University Press, New York, 2006.
H.T. MacGillivray, R.J. Dodd, Monte-Carlo Simulations of Galaxy Systems II: Static Properties for Galaxies in Rich Clusters, Astrophysics and Space Science, 83 (1982) 127-142.
H.T. MacGillivray, R.J. Dodd, B.V. McNally, J.F. Lightfoot, H.G. Corwin Jr, S.R. Heathcote, Monte-Carlo Simulations of Galaxy Systems I: The Local Supercluster, Astrophysics and Space Science, 81 (1982) 231-250.
D.K. Umberger, J.D. Farmer, I.I. Satija, A Universal Strange Attractor Underlying the Quasiperiodic Transition to Chaos, Physics Letters A, 114 (1986) 341-345.
P. Landau, K. Binder, A Guide to Monte Carlo Simulations in Statistical Physics, 2nd ed., Cambridge University Press, Cambridge, 2005.
A.D. Rollett, P. Manohar, The Monte Carlo Method, in: D. Raabe, F. Roters, F. Barlat, C. Long-Qing (Eds.) Continuum Scale Simulation of Engineering Materials, Wiley-VCH, Strauss GmbH, Morlenbach, 2004, pp. 77-114.

Deterministic, rule-based evolution

[37] K. Janssens, Cellular Automata, in: K.G.F. Janssens, D. Raabe, E. Kozeschnik, M.A. Miodownik, B. Nestler (Eds.) Computational Materials Engineering: An Introduction to Microstructure Evolution, Elsevier, Inc., Burlington, MA, 2007, pp. 109-150.
[38] D. Raabe, Cellular, Lattice Gas, and Boltzmann Automata, in: D. Raabe, F. Roters, F. Barlat, L.-Q. Chen (Eds.) Continuum Scale Simulation of Engineering Materials: Fundamentals-Microstructures-Process Applications, Wiley-VCH, Strauss GmbH, 2004, pp. 57-76.
[39] D. Raabe, Yield Surface Simulation for Partially Recrystallized Aluminum Polycrystals on the Basis of Spatially Discrete Data, Computational Materials Science, 19 (2000) 13-26.
[40] D. Raabe, Mesoscale Simulation of Recrystallization Textures and Microstructures, Advanced Engineering Materials, 3 (2001) 745-752.

Grain Growth (kMC)

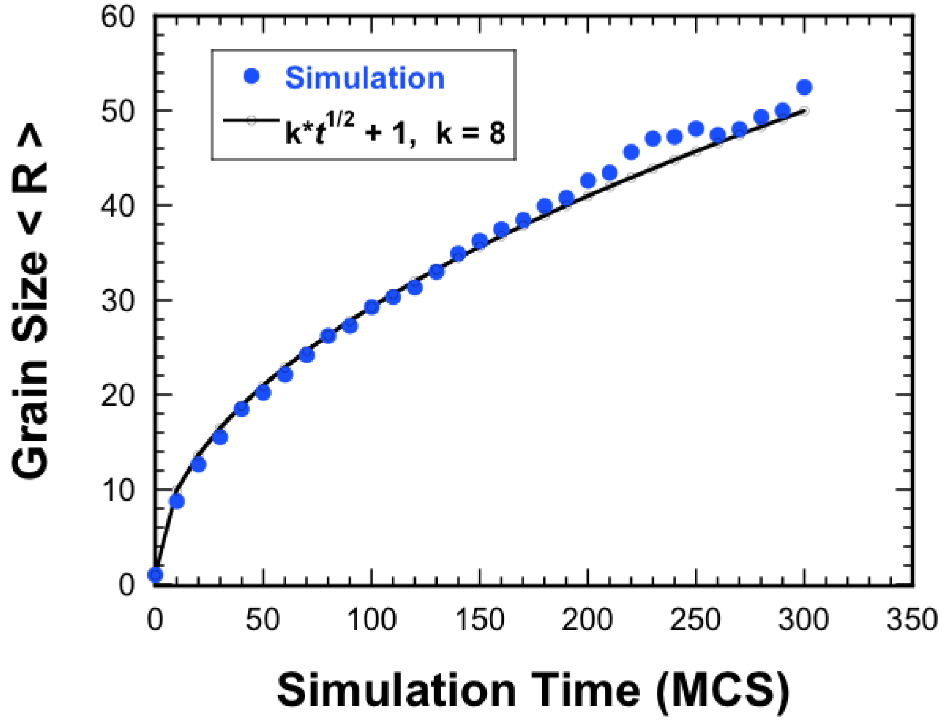

$$E_{GG} = \frac{1}{2}\sum_{i=1}^{N}\sum_{j=1}^{neigh}[1-\delta(q_i, q_j)]$$

$$P = \begin{cases} \exp\left(\frac{-\Delta E}{k_B T_S}\right) & if \ \Delta E > 0 \\ 1 & if \ \Delta E \leq 0 \end{cases}$$

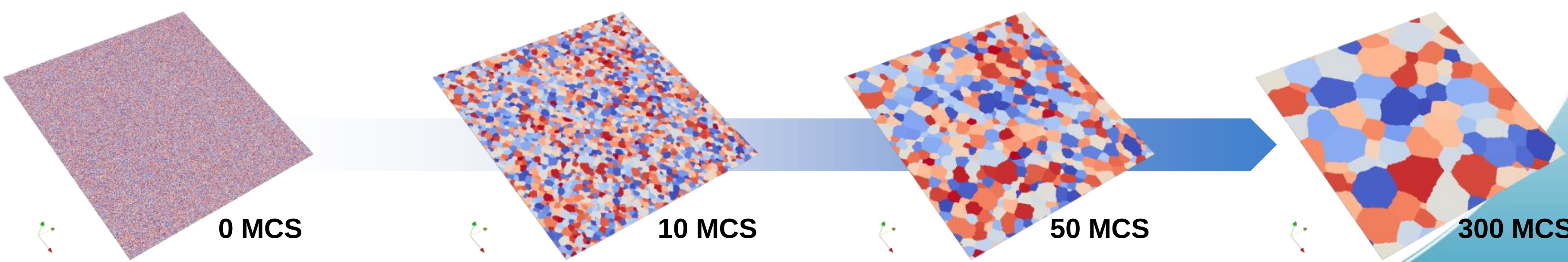

Sandia National Laboratories

Recrystallization (C.A.)

Binary Energy Case [e = 1 or 0]
2Dimensional, Site Saturated

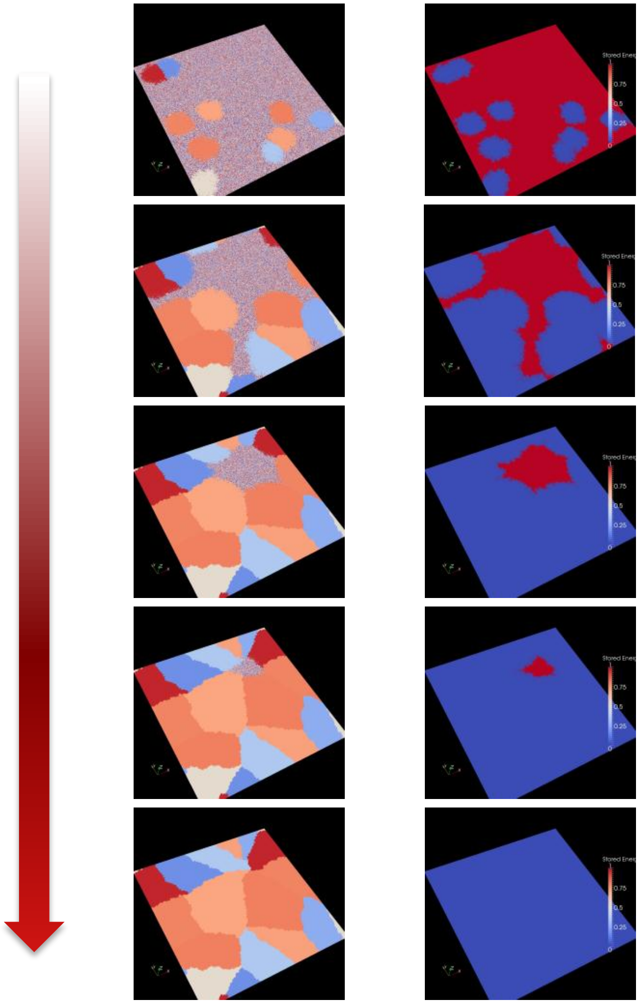

spins stored energy

$$if\ \Omega_i < \Omega_j^{initial} \begin{cases} \Omega_j = \Omega_i \\ spin_j = spin_i \end{cases}$$

Although the CA approach is entirely stored energy dependent, changes of spin accompany all recrystallization events. Should a neighboring grain possess a higher energy, under recrystallization, that grain will inherit both the lower stored energy and spin of the adjacent grain

$$\Delta E_{i,RC} = \Omega_i^{final} - \Omega_i^{initial} \qquad P = \begin{cases} 0 & if\ \Delta E > 0 \\ \dfrac{\left|\Delta E_{i,RC}\right|}{\Omega^{MAX}} & if\ \Delta E \leq 0 \end{cases}$$

Sandia National Laboratories

Recrystallization (C.A.)

Binary Energy Case [e = 1 or 0]
2Dimensional, Site Saturated

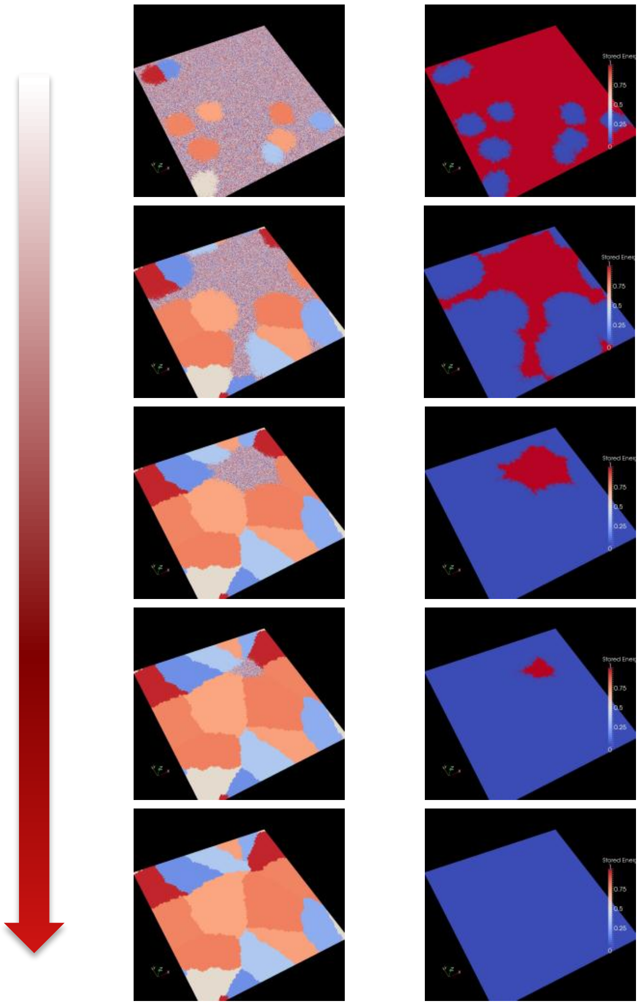

spins stored energy

$$Spins = 100$$

$$Total\ Sites = 250\,000$$

$$Total\ N_{accepted} = 247\,418$$

$$(1-f) = \frac{(Total\ N_{accepted} - N_{accepted})}{Total\ N_{accepted}}$$

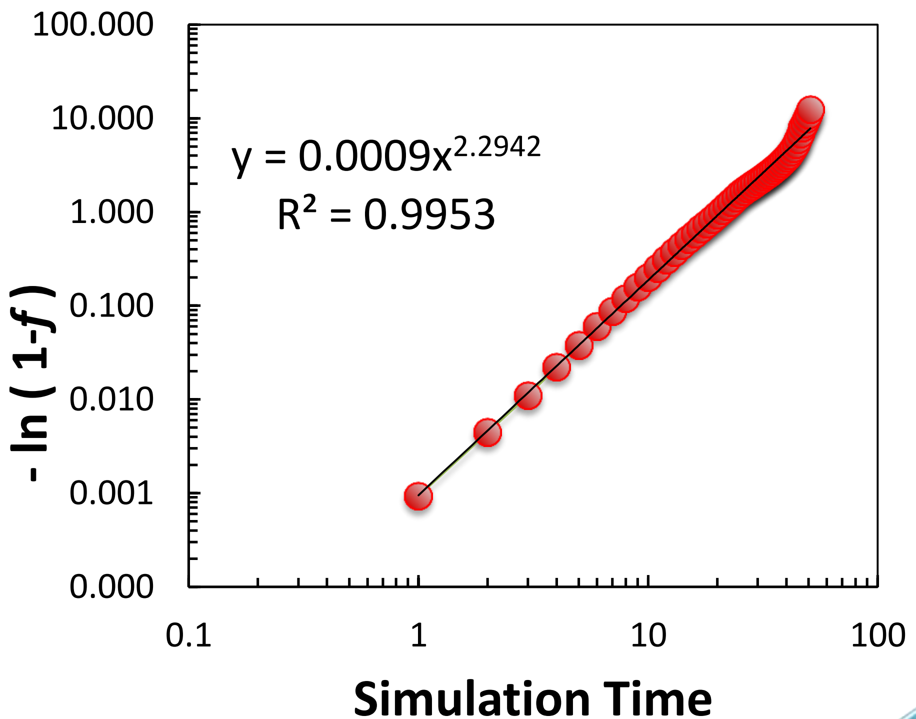

Energy Accumulation & Nucleation

$$\Omega(i,t+1) = \Omega(t) + \Delta t\left(uniform\ e_i\right)$$

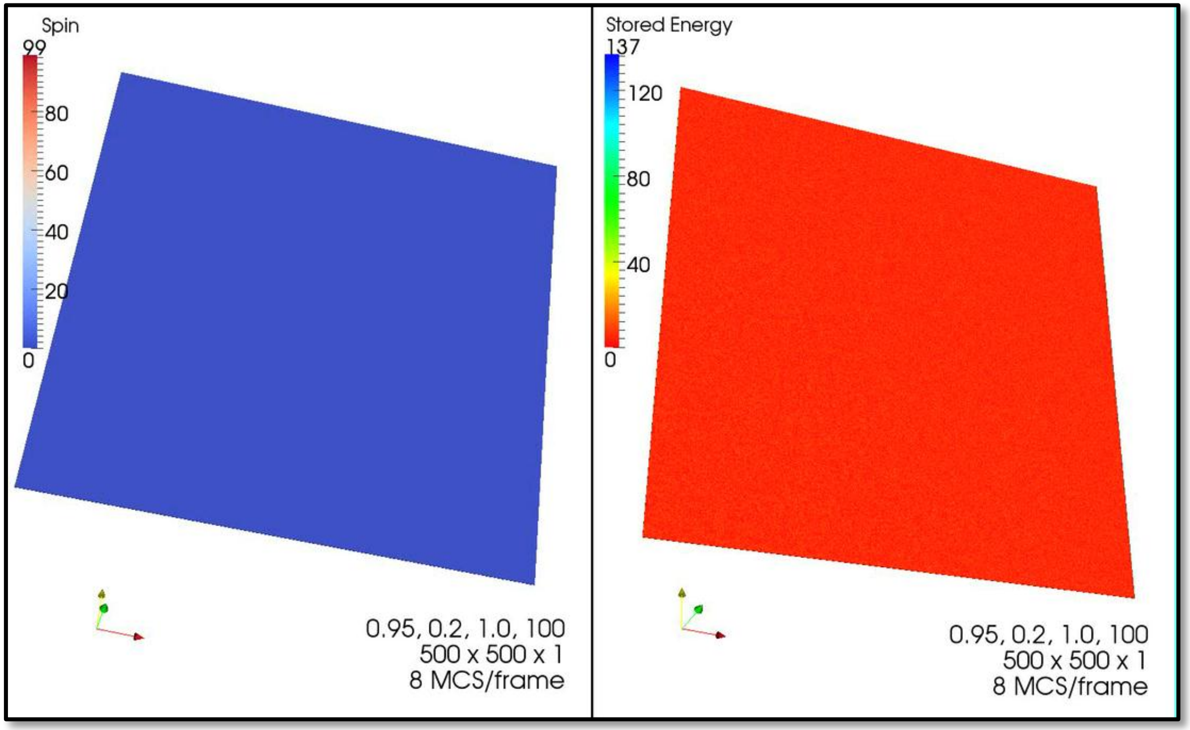

Damage energy is continually supplied to the system with time

Nuclei are introduced to the system in time and space according to the system's maximum stored energy

Newly introduced nuclei decrease local and global system energy

Effects on System Energy & Grain Size

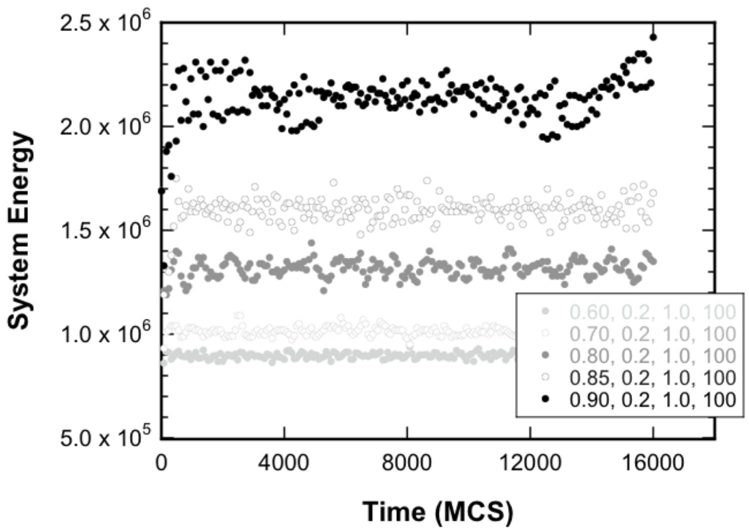

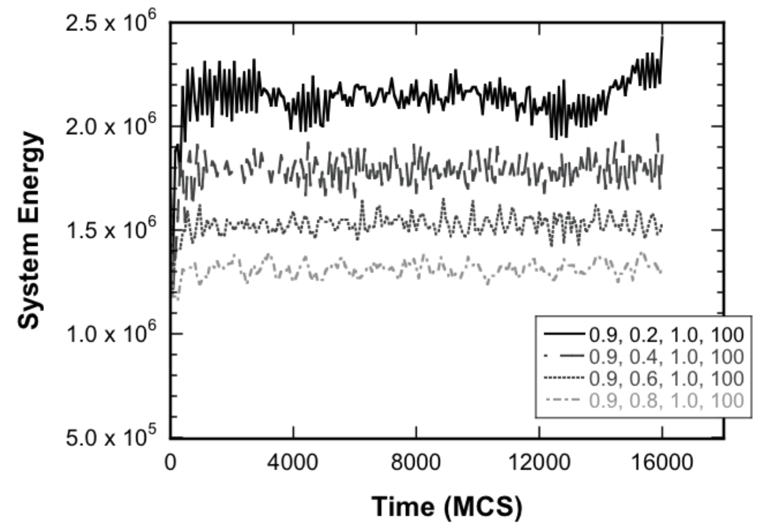

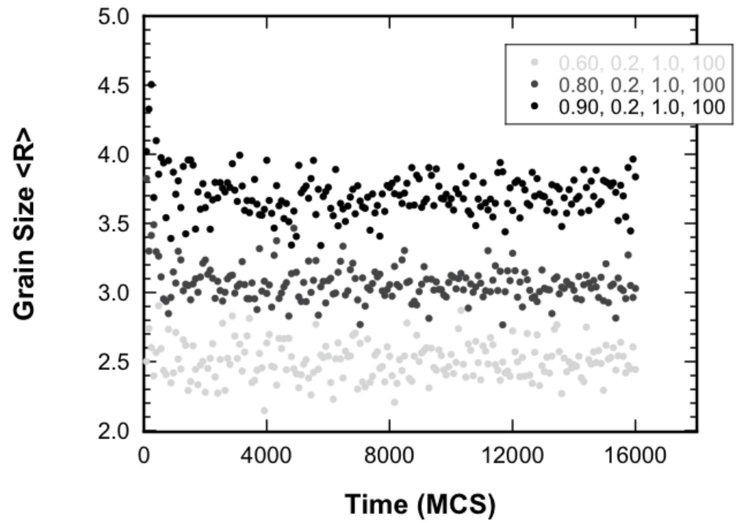

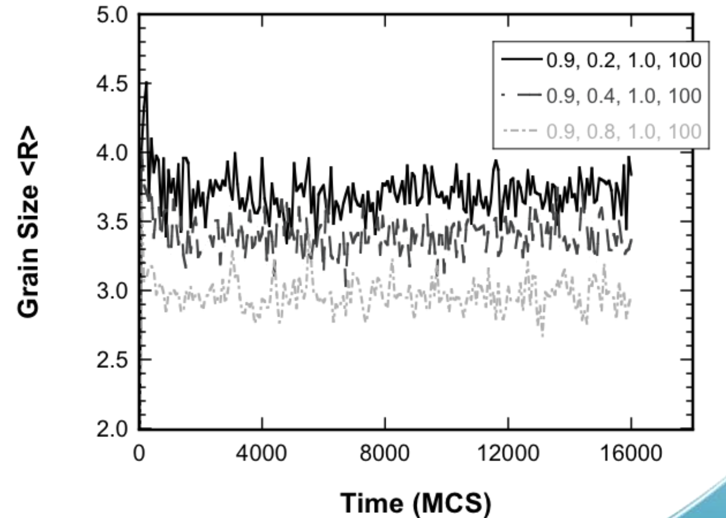

Legend notation: (1) threshold, (2) nucleation rate, (3) % grain growth , (4) % recrystallization

Hybrid Algorithm

$$\Omega(i,t+1) = \Omega(t) + \Delta t\left(r_i\right)$$

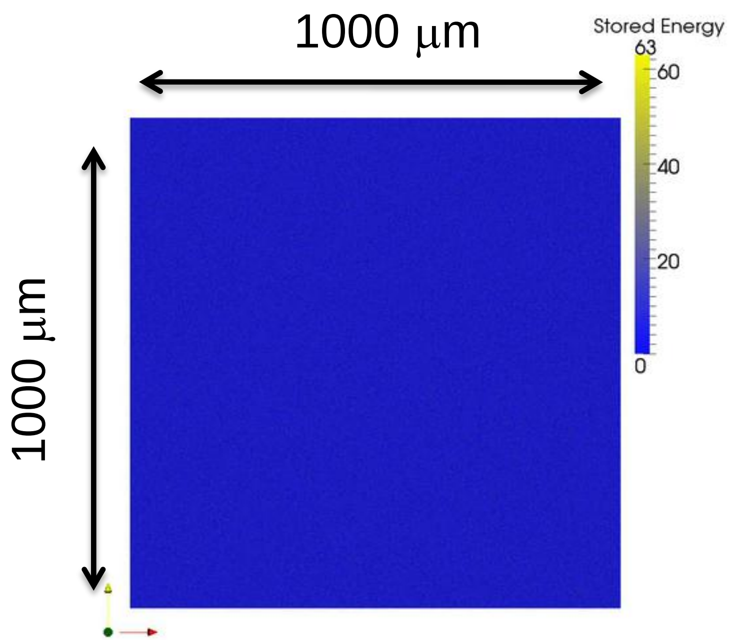

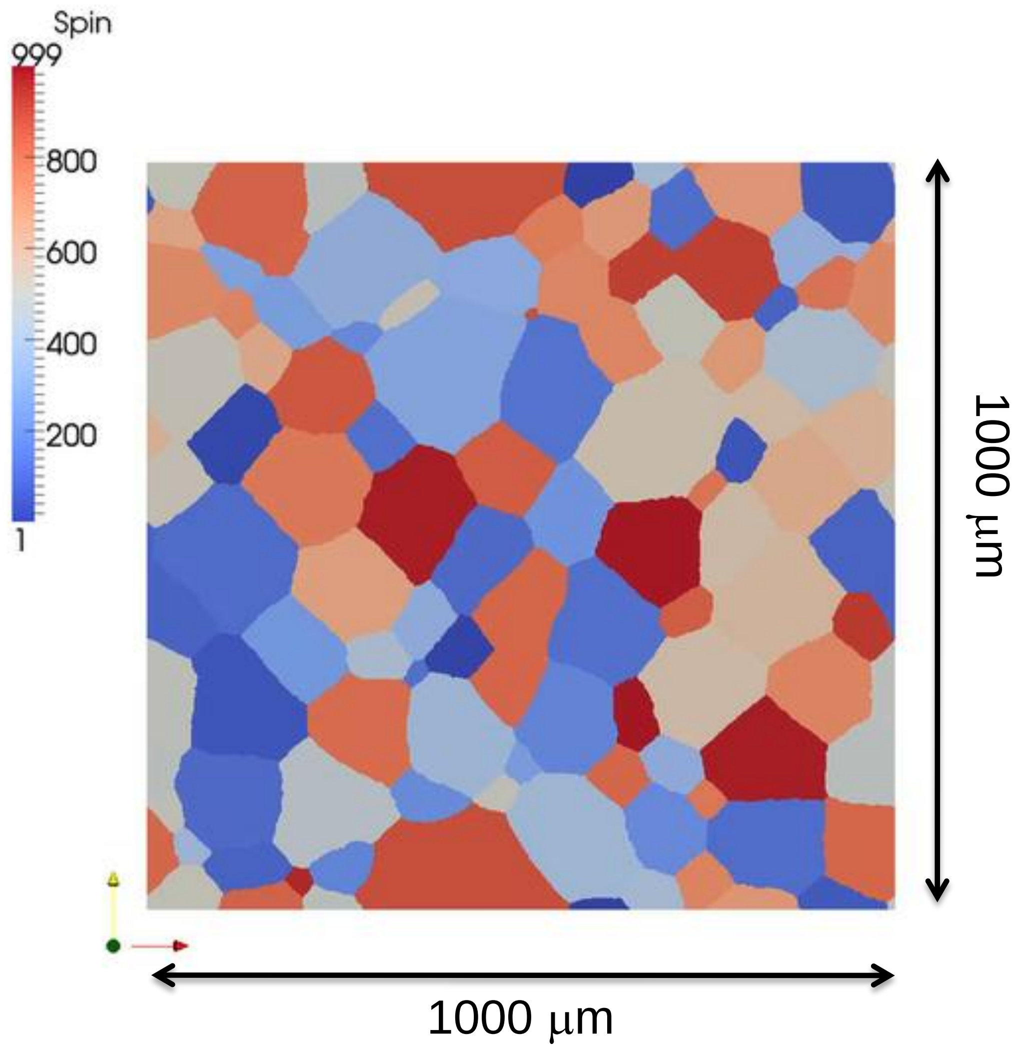

8 MCS / frame
1000 spins
1000 x 1000 x 1
Initial Grain Size <R> = 100
Average <R> During Recrystallization = 5

Representative Volume Element (RVE)

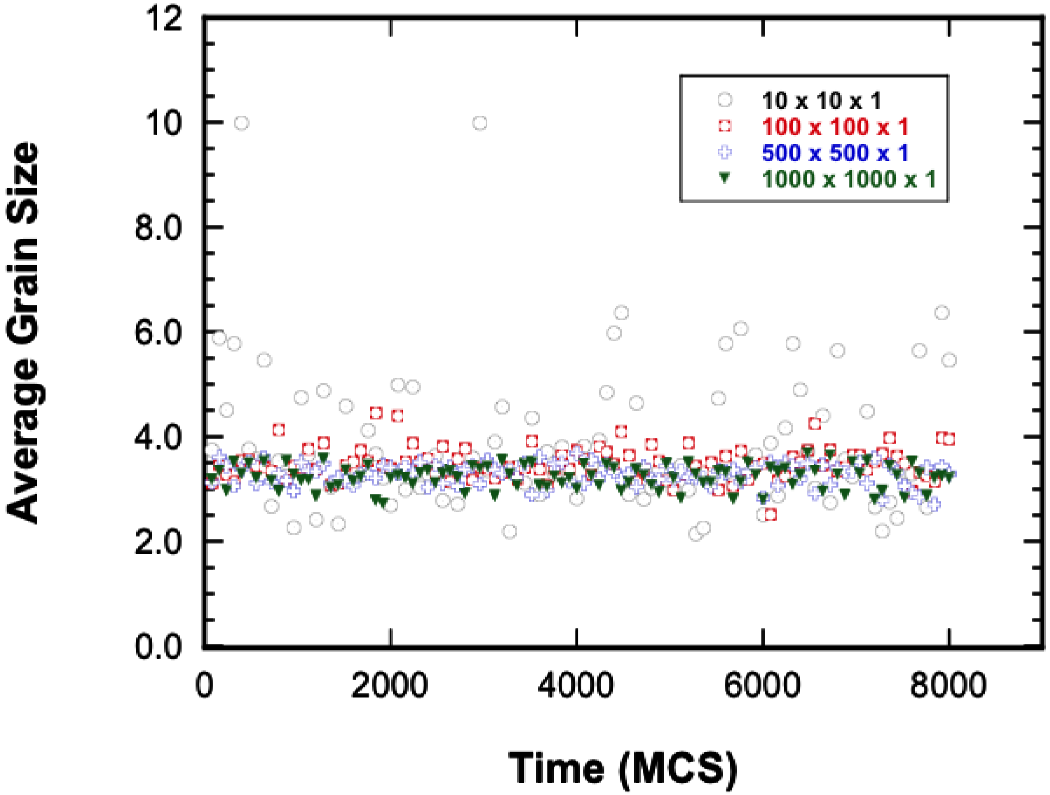

	AVG. <R>	ST. DEV
10^2	3.99	1.61
100^2	3.49	0.31
500^2	3.29	0.20
1000^2	3.24	0.22

Future Work

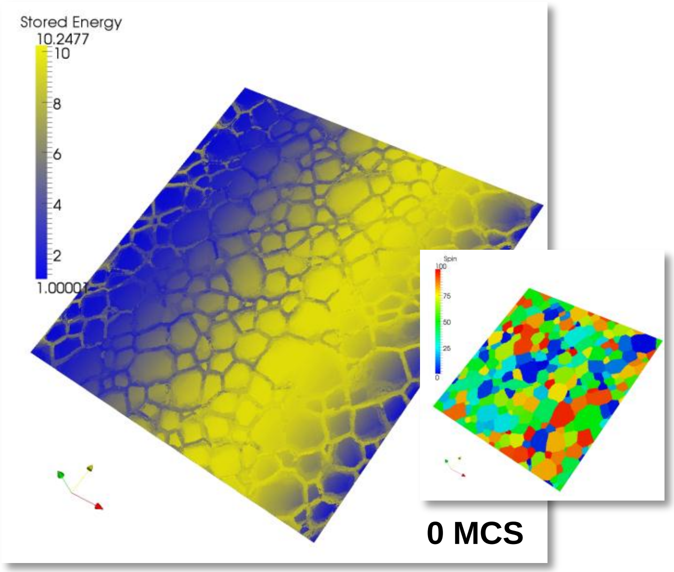

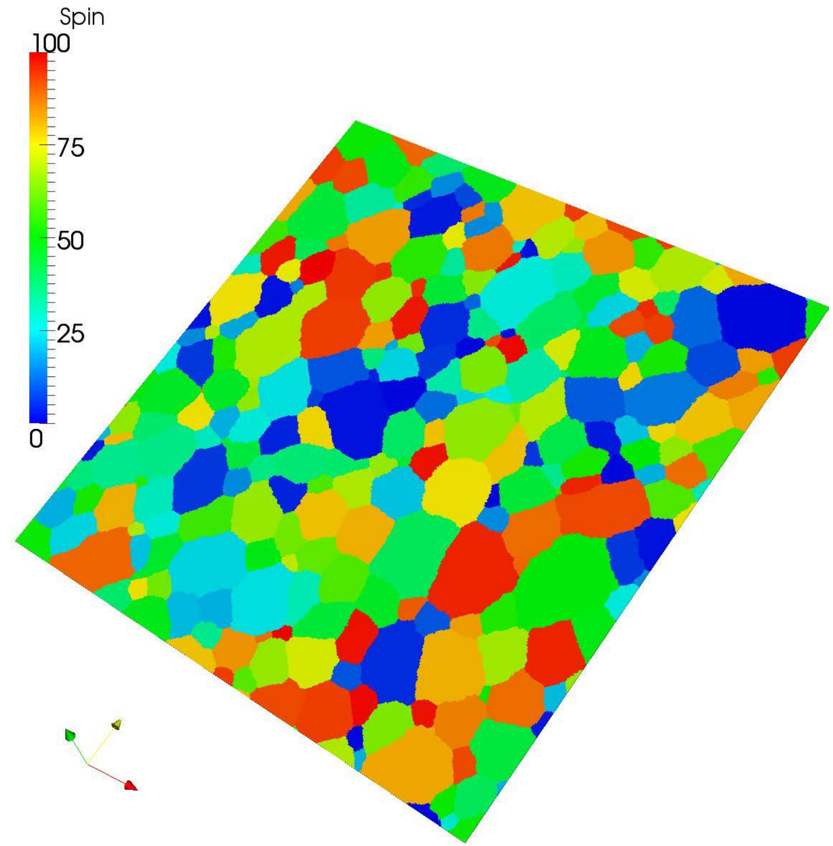

- Future work will focus on ascribing a damage accumulation which is both a function of position and time
- Toward a more realistic description of a nuclear fuel microstructure to include porosity, pore migration, variable boundary mobility and thermal gradients

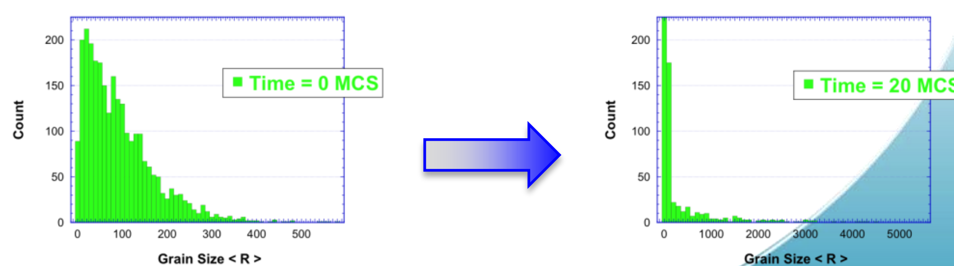

Sandia National Laboratories

Conclusions

A hybrid model combining kinetic Monte Carlo and Cellular Automata can successfully demonstrate dynamic recrystallization for basic description of microstructural evolution in nuclear fuels.

Increases in nucleation threshold, result in increased nominal system energy and higher average grain size, while increases in nucleation rate result in lower nominal system energy and lower average grain size.

The hybrid algorithm effectively provides characteristic trends in grain size, relative scaling and microstructural evolution with abbreviated domains down to 100^2 elements.

Questions